

Testing the nested light-cone Bethe equations of the $AdS_5 \times S^5$ superstring

Alexander Hentschel, Jan Plefka and Per Sundin

*Humboldt-Universität zu Berlin, Institut für Physik,
Newtonstraße 15, D-12489 Berlin, Germany*

alexander.hentschel, jan.plefka, per.sundin@physik.hu-berlin.de

ABSTRACT: We perform a detailed test of the quantum integrability of the $AdS_5 \times S^5$ superstring in uniform light-cone gauge in its near plane-wave limit. For this we establish the form of the general nested light-cone Bethe equations for the quantum string from the long range $\mathfrak{psu}(2, 2|4)$ Bethe equations of Beisert and Staudacher. Moreover the scheme for translating excited string states into Bethe root excitations is given. We then confront the direct perturbative diagonalization of the light-cone string Hamiltonian in the near plane-wave limit with the energy spectrum obtained from the general nested light-cone Bethe equations in various higher rank sectors. The analysis is performed both analytically and numerically up to the level of six impurity states and subsectors of maximal rank four. We find perfect agreement in all cases lending strong support to the quantum integrability of the $AdS_5 \times S^5$ superstring.

Contents

1. Introduction	2
2. The Superstring on $\text{AdS}_5 \times \text{S}^5$	4
2.1 Hamiltonian in uniform light-cone gauge	4
3. The light-cone Bethe equations for general sectors	6
4. Large P_+ expansion	12
4.1 Non-confluent mode numbers	12
4.2 Confluent mode numbers	13
4.3 Bethe equations for the smaller spin chains	14
5. Comparing the Bethe equations with string theory	15
5.1 General structure of solutions	15
5.2 The $\mathfrak{su}(1 2)$ sector	16
5.2.1 Two impurities	16
5.2.2 Three impurities, distinct mode numbers	17
5.2.3 Three impurities, confluent mode numbers	18
5.3 The $\mathfrak{su}(1, 1 2)$ sector	19
5.3.1 Two impurities	19
5.3.2 Three impurities, distinct mode numbers	20
5.3.3 Three impurities, confluent mode numbers	21
5.3.4 Higher impurities	22
5.4 The $\mathfrak{su}(2 3)$ sector	22
5.4.1 Two impurities	23
5.4.2 Higher impurities	23
6. Summary	25
A. Overview of the string results	25
A.1 The $\mathfrak{su}(2)$ sector	26
A.2 The $\mathfrak{sl}(2)$ sector	27
A.3 The $\mathfrak{su}(1 1)$ sector	27
A.4 The $\mathfrak{su}(1 2)$ sector	27
A.4.1 Two impurities	28
A.4.2 Three impurities with distinct modes	28
A.4.3 Three impurities with confluent modes	28
A.5 The $\mathfrak{su}(1, 1 2)$ sector	29

A.5.1	Two impurities	29
A.5.2	Three impurities with confluent modes	29
A.6	The $\mathfrak{su}(2 3)$ sector	30
A.6.1	Two impurities	31
B.	Numerical results	31

1. Introduction

Determining the spectrum of the type IIB superstring on the maximally supersymmetric $AdS_5 \times S^5$ background [1] is of great interest, both in view of the AdS/CFT correspondence [2] and as a problem in its own right within string theory. The string spectrum should be equivalent to the spectrum of scaling dimensions of local composite operators in the dual $\mathcal{N} = 4$, $U(N)$ super Yang-Mills theory in the 't Hooft limit.

In the last four years tremendous progress on this question has been made upon exploiting the *assumed* property of integrability in the system, following the pioneering work of Minahan and Zarembo [3]¹. Here progress was largely driven by advances on the gauge theory side, where it is possible to map the perturbative spectral problem to the diagonalization of a corresponding super spin chain [5]. Building upon one-loop studies [6] this finally led to the construction of a set of nested, asymptotic all-loop Bethe equations for the full model [7]. Moreover the underlying symmetry of the supergroup $PSU(2, 2|4)$ was shown to determine the S-matrix [8] of the system up to an overall phase or dressing factor [9]. As argued by Janik this abelian dressing factor can be constrained by crossing-invariance [10] pointing towards an underlying Hopf algebraic structure [11]. Recently a proposal for the full dressing factor was made [12] which remarkably agrees with the findings of an independent four loop computation [13] in the gauge theory.

Compared to these advances our understanding of the string side of the correspondence is less developed to date. The sigma-model describing the $AdS_5 \times S^5$ string is an integrable model [14] at the classical level and one certainly hopes this to remain true also in the quantum theory. In [15] a solitonic solution of the classical string was identified as the dual object to the spin chain magnon, reproducing the spin chain dispersion relation in the strong 'tHooft coupling limit. While it is unclear at present how to attack an exact quantization of the $AdS_5 \times S^5$ string, the problem is feasible upon consideration of suitable limits of the background geometry and perturbative expansions around them. The most prominent example is the Penrose limit to a

¹For reviews see [4].

plane-wave background [16], where the string sigma model becomes a free massive theory on the worldsheet. Here the first corrections to the plane-wave geometry can be treated perturbatively and the leading corrections to the plane-wave spectrum was established in a series of papers [17, 18]. Moreover Arutyunov, Frolov and Staudacher [20] showed that these corrections are reproduced from a set of quantum string Bethe equations in certain rank one subsectors, which have also been generalized to the full model in [7]. A central question in the analysis of the $AdS_5 \times S^5$ superstring is that of a convenient gauge choice for the worldsheet diffeomorphisms and kappa symmetry. Building upon previous studies in reduced subsectors [21, 22] it was realized in [23] that a uniform light-cone gauge employing the sum and difference of the global time coordinate and an angle on the S^5 as light-cone coordinates, along with a suitable kappa-symmetry gauge, simplifies the problem considerably. In that paper the exact light-cone Hamiltonian of the $AdS_5 \times S^5$ string was established and the near plane-wave limit was performed, i.e. the limit of large light-cone momentum P_+ with $\sqrt{\lambda}/P_+$ held fixed. The resulting corrections at leading order $1/P_+$ in the light-cone energy were established and a set of “light-cone” Bethe equations was proposed, which reproduced these energy shifts in the rank one subsectors $\mathfrak{su}(2)$, $\mathfrak{sl}(2)$ and $\mathfrak{su}(1|1)$. Curiously, the form of these Bethe equations is simpler than the gauge theory inspired ones [20] in that they come with a dressing factor equal to unity. This statement is expected to hold, of course, only modulo unexplored terms at higher order in $1/P_+$. The residual symmetry structure of the light-cone gauged superstring was investigated in [24] and in [25] assuming integrability a Zamolodchikov-Fadeev algebra was introduced for the superstring.

One aim of the present paper is to clarify the connection of the light-cone Bethe equations to the “standard” gauge theory inspired Bethe equations of [20] and its generalization to the full higher rank system [7] including the latest dressing factor. The set of nested light-cone Bethe equations for general excitations of the near plane-wave superstring is derived and the translation scheme from string oscillator excitations to Bethe root excitations is given. The energy shifts obtained from solving the nested light-cone Bethe equations is confronted with the results of an explicit diagonalization of the interacting near-plane wave Hamiltonian at leading order perturbation theory. This analysis is performed in higher rank subsectors of $\mathfrak{su}(1|2)$, $\mathfrak{su}(1, 1|2)$ and $\mathfrak{su}(2|3)$ analytically for lower excitation numbers and numerically for up to six excitations. Perfect agreement is found in all cases, thus constituting a strong check of the quantum integrability of the $AdS_5 \times S^5$ superstring. If true the spectrum of the $AdS_5 \times S^5$ superstring – at least in the long string limit $P_+ \gg 1$ with all orders in a $1/P_+$ expansion included – should be given by the solutions of the general nested light-cone Bethe equations augmented by the conjectured dressing phase of [12].

Our analysis is complementary to the direct computation of the worldsheet S-matrix reported in [26], see also [27]. In [26] the emergence of the two particle S-

matrix of Beisert [9] at leading order in $1/P_+$ was confirmed, which is known to lead to the nested asymptotic Bethe equations of [7]. This finding is a necessary but not sufficient condition for the integrability of the quantum $AdS_5 \times S^5$ superstring, which would imply factorization of multi-particle scattering and the absence of particle production. Indeed the factorization of three particle scattering in the bosonic sector was demonstrated in the S-matrix approach of [26]. Our paper now provides a stringent test of the factorization property in larger sectors and at higher particle excitation numbers.

The plan of the paper is as follows. We begin by recalling the necessary facts of the uniform light-cone gauged $AdS_5 \times S^5$ superstring in the near plane wave limit in chapter two. Chapter three is then devoted to the derivation of the nested light-cone Bethe equations for the full excitation structure. Moreover we present a string oscillator/Dynkin node excitation dictionary to translate the string into the Bethe equation language. In chapter four we discuss the large P_+ limit of this set of nested equations and present the emerging coupled polynomial equations for the Bethe roots which need to be solved. Explicit solutions are carried out for a number of subsectors and impurity numbers up to six (both with distinct and confluent mode numbers) in chapter five. The computations on the string side have been relegated to the appendix.

2. The Superstring on $AdS_5 \times S^5$

2.1 Hamiltonian in uniform light-cone gauge

In [23] an exact gauge fixed Lagrangian of the Green-Schwarz Superstring on an $AdS_5 \times S^5$ background was constructed in the uniform light-cone gauge [21, 22]. The associated light-cone Hamiltonian is given by $\mathcal{H} = -P_-$ where $P_{\pm} := J \pm E$. Here J denotes the angular momentum on S^5 and E the global space-time energy.

Due to its nonlinearity an exact quantization of this system is unknown, nevertheless the Hamiltonian of [23] allows for a perturbative quantization in the near plane wave limit, where P_+ is taken to be large with $\tilde{\lambda} := \frac{4\lambda}{P_+}$ held fixed. Using this approach the quantized perturbative Hamiltonian has been computed up to next-to-leading order in a $1/P_+$ expansion

$$\mathcal{H} = \mathcal{H}_2 + \frac{1}{P_+} \mathcal{H}_4 + \mathcal{O}(P_+^{-2}) \quad (2.1)$$

The dynamical fields are given by the transverse eight fermionic and eight bosonic fields. We will use the following decomposition of the eight complex bosonic fields Z_a, Y_a and their corresponding canonical momenta P_a^z, P_a^y following the conventions

in [23]

$$\begin{aligned}
Z_a(\tau, \sigma) &= \sum_n e^{in\sigma} Z_{a,n}(\tau) & P_a^z(\tau, \sigma) &= \sum_n e^{in\sigma} P_{a,n}^z(\tau) \\
Z_{a,n} &= \frac{1}{i\sqrt{\omega_n}} (\beta_{a,n}^+ - \beta_{5-a,-n}^-) & P_{a,n}^z &= \frac{\sqrt{\omega_n}}{2} (\beta_{a,n}^+ + \beta_{5-a,-n}^-) \\
Y_a(\tau, \sigma) &= \sum_n e^{in\sigma} Y_{a,n}(\tau) & P_a^y(\tau, \sigma) &= \sum_n e^{in\sigma} P_{a,n}^y(\tau) \\
Y_{a,n} &= \frac{1}{i\sqrt{\omega_n}} (\alpha_{a,n}^+ - \alpha_{5-a,-n}^-) & P_{a,n}^y &= \frac{\sqrt{\omega_n}}{2} (\alpha_{a,n}^+ + \alpha_{5-a,-n}^-), \tag{2.2}
\end{aligned}$$

where the frequency ω_n is defined as

$$\omega_n = \sqrt{1 + \tilde{\lambda} n^2}. \tag{2.3}$$

The decomposition has been chosen so that the creation and annihilation operators obey canonical commutation relations

$$[\alpha_{a,n}^-, \alpha_{b,m}^+] = \delta_{a,b} \delta_{n,m} = [\beta_{a,n}^-, \beta_{b,m}^+], \tag{2.4}$$

where $a \in \{1, 2, 3, 4\}$ is the flavor index and n, m are the mode numbers which are subject to the level matching condition

$$\sum_{j=1}^{K_4} m_j = 0, \tag{2.5}$$

where K_4 denotes the total number of excitations. The mode decompositions for the fermions² are:

$$\begin{aligned}
\eta(\tau, \sigma) &= \sum_n e^{in\sigma} \eta_n(\tau) & \theta(\tau, \sigma) &= \sum_n e^{in\sigma} \theta_n(\tau) \\
\eta_n &= f_n \eta_n^- + i g_n \eta_n^+ & \theta_n &= f_n \theta_n^- + i g_n \theta_n^+ \tag{2.6}
\end{aligned}$$

$$\text{with } \eta_k^- = \eta_{a,k}^- \Gamma_{5-a}, \quad \eta_k^+ = \eta_{a,k}^+ \Gamma_a, \quad \theta_k^- = \eta_{a,k}^- \Gamma_{5-a}, \quad \theta_k^+ = \eta_{a,k}^+ \Gamma_a. \tag{2.7}$$

Where the explicit representation of the Dirac matrices Γ_a is given in [23]. The functions f_m and g_m above are defined as

$$f_m = \sqrt{\frac{1}{2} \left(1 + \frac{1}{\omega_m}\right)}, \quad g_m = \frac{\kappa \sqrt{\tilde{\lambda} m}}{1 + \omega_m} f_m. \tag{2.8}$$

²For the sake of completeness the mode decomposition of the η -field is given in this chapter. It is not to be confused with the grading η_1, η_2 , which are used in section 3 to describe different choices of Dynkin diagrams for $\mathfrak{psu}(2, 2|4)$

Here $\kappa = \pm 1$ is the arbitrary relative sign between kinetic and Wess-Zumino term in the worldsheet action. The anti-commutators between the fermionic mode operators are then

$$\{\eta_{a,n}^-, \eta_{b,m}^+\} = \delta_{a,b} \delta_{n,m} = \{\theta_{a,n}^-, \theta_{b,m}^+\}. \quad (2.9)$$

Using this oscillator representation, the leading order Hamiltonian becomes

$$\mathcal{H}_2 = \sum_n \omega_n (\theta_{a,n}^+ \theta_{a,n}^- + \eta_{a,n}^+ \eta_{a,n}^- + \beta_{a,n}^+ \beta_{a,n}^- + \alpha_{a,n}^+ \alpha_{a,n}^-). \quad (2.10)$$

The first order correction to this Hamiltonian is given by [23]

$$\mathcal{H}_4 = \mathcal{H}_{bb} + \mathcal{H}_{bf} + \mathcal{H}_{ff}(\theta) - \mathcal{H}_{ff}(\eta) \quad (2.11)$$

with
$$\mathcal{H}_{bb} = \frac{\tilde{\lambda}}{4} (Y'_{5-a} Y'_a Z'_{5-b} Z_b - Y_{5-a} Y_a Z'_{5-b} Z'_b + Z'_{5-a} Z'_a Z_{5-b} Z_b - Y'_{5-a} Y'_a Y_{5-b} Y_b) \quad (2.12)$$

$$\begin{aligned} \mathcal{H}_{bf} = \frac{\tilde{\lambda}}{4} \text{tr} \left[\right. & (Z_{5-a} Z_a - Y_{5-a} Y_a) (\eta'^{\dagger} \eta' + \theta'^{\dagger} \theta') \\ & - Z'_a Z_b [\Gamma_a, \Gamma_b] (\mathcal{P}_+ (\eta \eta'^{\dagger} - \eta' \eta^{\dagger}) - \mathcal{P}_- (\theta^{\dagger} \theta' - \theta'^{\dagger} \theta)) \\ & + Y'_a Y'_b [\Gamma_a, \Gamma_b] (-\mathcal{P}_- (\eta^{\dagger} \eta' - \eta'^{\dagger} \eta) - \mathcal{P}_+ (\theta \theta'^{\dagger} - \theta'^{\dagger} \theta)) \\ & - \frac{i\kappa}{\sqrt{\tilde{\lambda}}} (Z_a P_b^z)' [\Gamma_a, \Gamma_b] (\mathcal{P}_+ (\eta^{\dagger} \eta^{\dagger} + \eta \eta) + \mathcal{P}_- (\theta^{\dagger} \theta^{\dagger} + \theta \theta)) \\ & + \frac{i\kappa}{\sqrt{\tilde{\lambda}}} (Y_a P_b^y)' [\Gamma_a, \Gamma_b] (\mathcal{P}_- (\eta^{\dagger} \eta^{\dagger} + \eta \eta) + \mathcal{P}_+ (\theta^{\dagger} \theta^{\dagger} + \theta \theta)) \\ & \left. + 8i Z_a Y_b (-\mathcal{P}_- \Gamma_a \eta' \Gamma_b \theta' + \mathcal{P}_+ \Gamma_a \theta'^{\dagger} \Gamma_b \eta'^{\dagger}) \right] \quad (2.13) \end{aligned}$$

$$\mathcal{H}_{ff}(\eta) = \frac{\tilde{\lambda}}{4} \text{tr} \left[\Gamma_5 (\eta'^{\dagger} \eta \eta'^{\dagger} \eta + \eta^{\dagger} \eta' \eta^{\dagger} \eta' + \eta'^{\dagger} \eta^{\dagger} \eta'^{\dagger} \eta^{\dagger} + \eta' \eta \eta' \eta) \right]. \quad (2.14)$$

This is the Hamiltonian for which we will determine the energy shifts δP_- of the free, degenerate eigenstates $|\psi_{0,n}\rangle$ with $\mathcal{H}_2 |\psi_{0,n}\rangle = -(P_-)_0 |\psi_{0,n}\rangle$ by diagonalizing the matrix $\langle \psi_{0,n} | \mathcal{H}_4 | \psi_{0,m} \rangle$. These will then be compared to the energies resulting from the proposed light-cone Bethe equations. Due to the complexity of the Hamiltonian it is often hard to obtain analytical results for these energy shifts in larger sectors with more than a few number of excitations. We will then have to resort to numerical considerations.

3. The light-cone Bethe equations for general sectors

In an inspiring paper [7] the long range gauge and string theory Bethe equations were proposed for the full $\mathfrak{psu}(2, 2|4)$ sector. This proposal was based on a coordinate space, nested Bethe ansatz of the smaller $\mathfrak{su}(1, 1|2)$ sector, a construction later on

[9] generalized to $\mathfrak{su}(2|3)$. See [19] for a recent study of the problem employing the algebraic Bethe ansatz. We shall start our analysis from the full set of $\mathfrak{psu}(2,2|4)$ Bethe equations proposed in [7] in table 5 and adapt them to a language suitable for the light-cone gauge and large P_+ expansion performed in string theory [23]. This will set the basis for the subsequent comparison to the explicit diagonalization of the worldsheet Hamiltonian (2.11).

The proposed set of Bethe equations for the spectral parameters $x_{i,k}$ of Beisert and Staudacher [7] for the full model can be brought into the form

$$1 = \prod_{j=1}^{K_4} \frac{x_{4,k}^+}{x_{4,k}^-} \quad (3.1)$$

$$1 = \prod_{\substack{j=1 \\ j \neq k}}^{K_2} \frac{u_{2,k} - u_{2,j} - i\eta_1}{u_{2,k} - u_{2,j} + i\eta_1} \prod_{j=1}^{K_3+K_1} \frac{u_{2,k} - u_{3,j} + \frac{i}{2}\eta_1}{u_{2,k} - u_{3,j} - \frac{i}{2}\eta_1} \quad (3.2)$$

$$1 = \prod_{j=1}^{K_2} \frac{u_{3,k} - u_{2,j} + \frac{i}{2}\eta_1}{u_{3,k} - u_{2,j} - \frac{i}{2}\eta_1} \prod_{j=1}^{K_4} \frac{x_{4,j}^{+\eta_1} - x_{3,k}}{x_{4,j}^{-\eta_1} - x_{3,k}} \quad (3.3)$$

$$1 = \left(\frac{x_{4,k}^-}{x_{4,k}^+} \right)^{L - \eta_1 K_1 - \eta_2 K_7} \prod_{\substack{j=1 \\ j \neq k}}^{K_4} \left(\frac{x_{4,k}^{+\eta_1} - x_{4,j}^{-\eta_1}}{x_{4,k}^{-\eta_2} - x_{4,j}^{+\eta_2}} \frac{1 - g^2 / (x_{4,k}^+ x_{4,j}^-)}{1 - g^2 / (x_{4,k}^- x_{4,j}^+)} S_0^2 \right) \\ \times \prod_{j=1}^{K_3+K_1} \frac{x_{4,k}^{-\eta_1} - x_{3,j}}{x_{4,k}^{+\eta_1} - x_{3,j}} \prod_{j=1}^{K_5+K_7} \frac{x_{4,k}^{-\eta_2} - x_{5,j}}{x_{4,k}^{+\eta_2} - x_{5,j}} \quad (3.4)$$

$$1 = \prod_{j=1}^{K_6} \frac{u_{5,k} - u_{6,j} + \frac{i}{2}\eta_2}{u_{5,k} - u_{6,j} - \frac{i}{2}\eta_2} \prod_{j=1}^{K_4} \frac{x_{4,j}^{+\eta_2} - x_{5,k}}{x_{4,j}^{-\eta_2} - x_{5,k}} \quad (3.5)$$

$$1 = \prod_{\substack{j=1 \\ j \neq k}}^{K_6} \frac{u_{6,k} - u_{6,j} - i\eta_2}{u_{6,k} - u_{6,j} + i\eta_2} \prod_{j=1}^{K_5+K_7} \frac{u_{6,k} - u_{5,j} + \frac{i}{2}\eta_2}{u_{6,k} - u_{5,j} - \frac{i}{2}\eta_2}. \quad (3.6)$$

In the above the variables $u_{i,k}$ are defined by $u_{i,k} = x_{i,k} + g^2 \frac{1}{x_{i,k}}$ and the Bethe roots $x_{n,k}$ come with the multiplicities

$$x_{2,k} : k = 1, \dots, K_2 \quad x_{3,k} : k = 1, \dots, (K_1 + K_3) \quad x_{4,k}^\pm : k = 1, \dots, K_4 \\ x_{5,k} : k = 1, \dots, (K_5 + K_7) \quad x_{6,k} : k = 1, \dots, K_6 \quad (3.7)$$

Moreover the spectral parameters $x_{4,k}^\pm$ are related to the magnon momenta p_k via

$$x_{4,k}^\pm = \frac{1}{4} \left(\cot \frac{p_k}{2} \pm i \right) \left(1 + \sqrt{1 + \frac{\lambda}{\pi^2} \sin^2 \frac{p_k}{2}} \right). \quad (3.8)$$

and coupling constant g^2 is given by

$$g := \frac{\sqrt{\lambda}}{4\pi} = \frac{\sqrt{\lambda} P_+}{8\pi}. \quad (3.9)$$

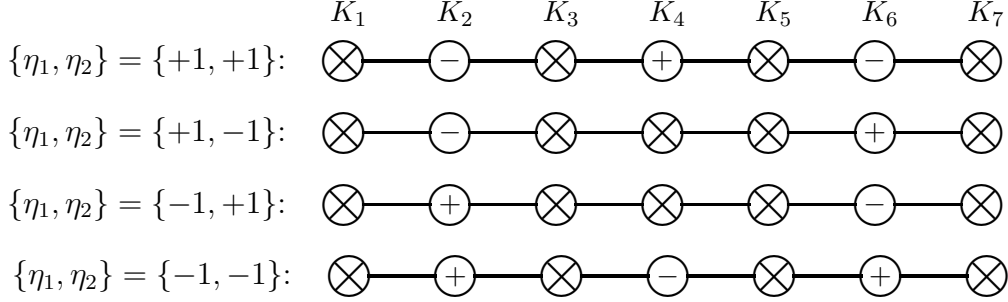


Figure 1: Four different choices of Dynkin diagrams of $\mathfrak{su}(2, 2|4)$ specified by the grading η_1 and η_2 . The signs in the white nodes indicate the sign of the diagonal elements of the Cartan matrix [7].

Note that we have chosen to write down the Bethe equations in a more compact “dynamically” transformed language. In order to convert (3.1)-(3.6) to the form found in table 5 of Beisert and Staudacher [7] one introduces the K_1 resp. K_7 roots $x_{1,k}$ and $x_{7,k}$ by splitting off the ‘upper’ $x_{3,k}$ and $x_{5,k}$ roots via

$$x_{1,k} := g^2/x_{3,K_3+k} \quad k = 1, \dots, K_1 \quad x_{7,k} := g^2/x_{5,K_5+k} \quad k = 1, \dots, K_7. \quad (3.10)$$

This coordinate renaming unfolds the equations associated to the fermionic roots (3.2) and (3.5) into two structurally new sets of K_1 and K_7 equations and removes the K_1 and K_7 dependent exponent in the central equation (3.4).

The first equation (3.1) of the form we will be using is the cyclicity constraint on the total momentum of the spin chain. The following $K_2 + (K_1 + K_3) + K_4 + (K_5 + K_7) + K_6$ equations in (3.2)-(3.6) determine the sets of Bethe roots $\{x_{2,k}, x_{3,k}, x_{4,k}^\pm, x_{5,k}, x_{6,k}\}$. Let us stress once more that it is only the combinations $(K_1 + K_3)$ and $(K_5 + K_7)$ which enter in the Bethe equations. Moreover the gradings η_1 and η_2 take the values ± 1 corresponding to four different choices of Dynkin diagrams for $\mathfrak{psu}(2, 2|4)$ as discussed in [7] see figure 1.

These four different choices of diagrams can be traced back to the derivation of the nested Bethe ansatz in the $\mathfrak{su}(1, 1|2)$ sector in the gauge theory spin chain language. In this sector there are four distinct excitations placed on a vacuum of \mathcal{Z} fields. These four excitations are the two bosonic \mathcal{X} and \mathcal{DZ} fields and the two fermionic \mathcal{U} and $\dot{\mathcal{U}}$ fields. In the nested Bethe ansatz [29] one selects one out of these four excitations as a second effective vacuum of a shorter spin chain, after having eliminated all the sites \mathcal{Z} from the original chain. Depending on this choice η_1, η_2 take the values ± 1 .

Finally, the undetermined function S_0^2 in (3.4) is the famous scalar dressing factor which is conjectured to take the form $S_0^2 = S_0^2(x_{4,k}, x_{4,j}) = e^{2i\theta(x_{4,k}, x_{4,j})}$ [20], where

$$\theta(x_{4,k}, x_{4,j}) = \sum_{r=2}^{\infty} \sum_{s=r+1}^{\infty} c_{r,s}(g) \left[q_r(x_{4,k}^\pm) q_s(x_{4,j}^\pm) - q_r(x_{4,j}^\pm) q_s(x_{4,k}^\pm) \right] \quad (3.11)$$

with the local conserved charge densities

$$q_r(x^\pm) = \frac{i}{r-1} g^{r-1} \left[\left(\frac{1}{x^+} \right)^{r-1} - \left(\frac{1}{x^-} \right)^{r-1} \right] \quad (3.12)$$

and to leading order

$$c_{r,s}(g) = g \left[\delta_{r+1,s} + \mathcal{O}(1/g) \right]. \quad (3.13)$$

In this paper, we shall only be interested in this leading order contribution, the AFS phase [20], where the phase factor may be summed [28] to yield

$$\begin{aligned} \theta_{kj} &= (x_j^+ - x_k^+) F(x_k^+ x_j^+) + (x_j^- - x_k^-) F(x_k^- x_j^-) \\ &\quad - (x_j^+ - x_k^-) F(x_k^- x_j^+) - (x_j^- - x_k^+) F(x_k^+ x_j^-), \end{aligned} \quad (3.14)$$

with

$$F(a) = \left(1 - \frac{g^2}{a}\right) \log\left(1 - \frac{g^2}{a}\right). \quad (3.15)$$

The string oscillator excitations are characterized by the values of four $U(1)$ charges (S_+, S_-, J_+, J_-) as introduced in [24]. They are related to the two spins $\{S_1, S_2\}$ on AdS_5 and two angular momenta $\{J_1, J_2\}$ on the S_5 via $S_\pm = S_1 \pm S_2$ and $J_\pm = J_1 \pm J_2$. The relationship between these and the excitation numbers $\{K_i\}$ in the Bethe equations are³

$$\begin{aligned} S_+ &= \eta_2 (K_5 + K_7) - (1 + \eta_2) K_6 + \frac{1}{2}(1 - \eta_2) K_4, \\ S_- &= \eta_1 (K_1 + K_3) - (1 + \eta_1) K_2 + \frac{1}{2}(1 - \eta_1) K_4, \\ J_+ &= -\eta_2 (K_5 + K_7) - (1 - \eta_2) K_6 + \frac{1}{2}(1 + \eta_2) K_4, \\ J_- &= -\eta_1 (K_1 + K_3) - (1 - \eta_1) K_2 + \frac{1}{2}(1 + \eta_1) K_4. \end{aligned}$$

Using these together with the (S_+, S_-, J_+, J_-) charge values for the string oscillators of table 9 (see also [24]) we can construct the excitation pattern for each oscillator, see table 1. For example, the excitations in the $\mathfrak{su}(1, 1|2)$ sector correspond to the following string oscillators,

$$\mathcal{X} \doteq \alpha_1^+, \quad \mathcal{DZ} \doteq \beta_1^+, \quad \mathcal{U} \doteq \theta_1^+, \quad \dot{\mathcal{U}} \doteq \eta_1^+. \quad (3.16)$$

These are the four fields which are picked out as a new vacuum in the smaller spin chains by specifying the values⁴ of the gradings η_1 and η_2 . The vacuum of \mathcal{Z} fields corresponds to the string ground state $|0\rangle$ with charge J .

³To make a connection to [7], we have $J_- = q_1, J_+ = q_2, S_- = s_1$ and $S_+ = s_2$. The two other charges, p and r are functions of the length of the spin chain, so in the large P_+ limit these are infinite.

⁴The field that is picked as the second vacuum in the nested Bethe ansatz only excites the middle node of the Dynkin diagram, so one immediately sees from the table which combinations of the gradings correspond to which choice of vacuum.

	$\mathbf{K}_1 + \mathbf{K}_3$	\mathbf{K}_2	\mathbf{K}_4	\mathbf{K}_6	$\mathbf{K}_5 + \mathbf{K}_7$	S_+	S_-	J_+	J_-
α_1^+	$0 + \frac{1}{2}(1 - \eta_1)$	0	1	0	$\frac{1}{2}(1 - \eta_2) + 0$	0	0	1	1
α_2^+	$\frac{1}{2}(1 + \eta_1) + 1$	1	1	0	$\frac{1}{2}(1 - \eta_2) + 0$	0	0	1	-1
α_3^+	$0 + \frac{1}{2}(1 - \eta_1)$	0	1	1	$1 + \frac{1}{2}(1 + \eta_2)$	0	0	-1	1
α_4^+	$\frac{1}{2}(1 + \eta_1) + 1$	1	1	1	$1 + \frac{1}{2}(1 + \eta_2)$	0	0	-1	-1
β_1^+	$0 + \frac{1}{2}(1 + \eta_1)$	0	1	0	$\frac{1}{2}(1 + \eta_2) + 0$	1	1	0	0
β_2^+	$\frac{1}{2}(1 - \eta_1) + 1$	1	1	0	$\frac{1}{2}(1 + \eta_2) + 0$	1	-1	0	0
β_3^+	$0 + \frac{1}{2}(1 + \eta_1)$	0	1	1	$1 + \frac{1}{2}(1 - \eta_2)$	-1	1	0	0
β_4^+	$\frac{1}{2}(1 - \eta_1) + 1$	1	1	1	$1 + \frac{1}{2}(1 - \eta_2)$	-1	-1	0	0
θ_1^+	$0 + \frac{1}{2}(1 + \eta_1)$	0	1	0	$\frac{1}{2}(1 - \eta_2) + 0$	0	1	1	0
θ_2^+	$\frac{1}{2}(1 - \eta_1) + 1$	1	1	0	$\frac{1}{2}(1 - \eta_2) + 0$	0	-1	1	0
θ_3^+	$0 + \frac{1}{2}(1 + \eta_1)$	0	1	1	$1 + \frac{1}{2}(1 + \eta_2)$	0	1	-1	0
θ_4^+	$\frac{1}{2}(1 - \eta_1) + 1$	1	1	1	$1 + \frac{1}{2}(1 + \eta_2)$	0	-1	-1	0
η_1^+	$0 + \frac{1}{2}(1 - \eta_1)$	0	1	0	$\frac{1}{2}(1 + \eta_2) + 0$	1	0	0	1
η_2^+	$\frac{1}{2}(1 + \eta_1) + 1$	1	1	0	$\frac{1}{2}(1 + \eta_2) + 0$	1	0	0	-1
η_3^+	$0 + \frac{1}{2}(1 - \eta_1)$	0	1	1	$1 + \frac{1}{2}(1 - \eta_2)$	-1	0	0	1
η_4^+	$\frac{1}{2}(1 + \eta_1) + 1$	1	1	1	$1 + \frac{1}{2}(1 - \eta_2)$	-1	0	0	-1

Table 1: The translation scheme of string oscillator excitations to the Dynkin node excitation numbers of the Bethe equations. We have also listed the space-time $U(1)$ charges J_{\pm} and S_{\pm} of the string oscillators. From this table we easily see which operators represent the middle node for the different choices of gradings. That is, $(\eta_1, \eta_2) = (+, +) : \alpha_1^+$, $(-, +) : \theta_1^+$, $(+, -) : \eta_1^+$ and $(-, -) : \beta_1^+$.

Let us stress that in the dictionary of table 1 a single string oscillator excitation does not corresponds to a single Dynkin node excitation, but rather to a five component excitation vector, with uniform $K_4 = 1$ entry. This is how the naive mismatch of 16 string oscillators versus 7 (or better 4) Dynkin node excitations is resolved: One should think of a string oscillator as being indexed by the space-time charge vector (S_+, S_-, J_+, J_-) or by the Dynkin vector $(K_1 + K_3, K_2, K_6, K_5 + K_7)$. These two labelings are equivalent and the one-to-one map between them is given in (3.16).

There are several things we need to do in order to translate the Bethe equations (3.1)-(3.6) into their light-cone form in order to make a direct comparison to uniform light-cone gauged, near plane-wave string theory. First of all, since the light-cone Hamiltonian is expanded in the large P_+ limit we need to express L in (3.4) in terms of the light-cone momenta. This can be done by using the expression for the eigenvalues of the dilatation operator and the J charge of S^5 [7],

$$\begin{aligned}
J &= L + \frac{1}{2}\eta_1(K_3 - K_1) - \frac{1}{4}(2 + \eta_1 + \eta_2)K_4 + \frac{1}{2}\eta_2(K_5 - K_7), \\
D &= L + \frac{1}{2}\eta_1(K_3 - K_1) + \frac{1}{4}(2 - \eta_1 - \eta_2)K_4 + \frac{1}{2}\eta_2(K_5 - K_7) + \delta D,
\end{aligned} \tag{3.17}$$

where the anomalous dimension δD reads

$$\delta D = 2g^2 \sum_{j=1}^{K_4} \left(\frac{i}{x_{4,j}^+} - \frac{i}{x_{4,j}^-} \right), \quad (3.18)$$

Using (3.17) we can write the light-cone momenta and energy as,

$$\begin{aligned} P_+ &= D + J \\ &= 2L + \eta_1(K_3 - K_1) - \frac{1}{2}(\eta_1 + \eta_2)K_4 + \eta_2(K_5 - K_7) + \delta D \\ P_- &= J - D = -K_4 - \delta D. \end{aligned} \quad (3.19)$$

Hence we see that the large P_+ limit discussed in the previous section corresponds to an infinitely long chain with a finite number of excitations. Using this, the central K_4 Bethe equations (3.4) become

$$\begin{aligned} \left(\frac{x_{4,k}^+}{x_{4,k}^-} \right)^{\frac{1}{2}P_+} &= \left(\frac{x_{4,k}^-}{x_{4,k}^+} \right)^{\frac{1}{2}(\frac{1}{2}(\eta_1 + \eta_2)K_4 - \eta_1(K_1 + K_3) - \eta_2(K_5 + K_7) - \delta D)} \\ &\times \prod_{\substack{j=1 \\ j \neq k}}^{K_4} \left(\frac{x_{4,k}^{+\eta_1} - x_{4,j}^{-\eta_1}}{x_{4,k}^{-\eta_2} - x_{4,j}^{+\eta_2}} \frac{1 - g^2/(x_{4,k}^+ x_{4,j}^-)}{1 - g^2/(x_{4,k}^- x_{4,j}^+)} S_0^2 \right) \prod_{j=1}^{K_3 + K_1} \frac{x_{4,k}^{-\eta_1} - x_{3,j}}{x_{4,k}^{+\eta_1} - x_{3,j}} \prod_{j=1}^{K_5 + K_7} \frac{x_{4,k}^{-\eta_2} - x_{5,j}}{x_{4,k}^{+\eta_2} - x_{5,j}}. \end{aligned} \quad (3.20)$$

We want to compare the spectrum up to $\mathcal{O}(\frac{1}{P_+^2})$ and to this order a nice thing happens. As a matter of fact, one can show using only the leading AFS piece of (3.13) that

$$\left(\frac{x_{4,k}^-}{x_{4,k}^+} \right)^{-\frac{1}{2}\delta D} \prod_{\substack{j=1 \\ j \neq k}}^{K_4} \left(\frac{1 - g^2/(x_{4,k}^+ x_{4,j}^-)}{1 - g^2/(x_{4,k}^- x_{4,j}^+)} S_0^2 \right) = 1 + \mathcal{O}\left(\frac{1}{P_+^3}\right) \quad (3.21)$$

holds, once one inserts the large P_+ expansion of p_k (to be established in (4.1) and (4.3)) as well as the relevant leading AFS contribution to the dressing factor S_0 of (3.13). Curiously enough, not only the $1/P_+$ contribution, but also the $1/P_+^2$ term vanishes in this expansion – the $1/P_+^3$ term is nonvanishing though. Therefore, to the order we are interested in, the light-cone Bethe equations are given by the previous equations of (3.1)-(3.6) with the central node K_4 Bethe equations (3.4) exchanged by the simpler dressing factor free form

$$\begin{aligned} \left(\frac{x_{4,k}^+}{x_{4,k}^-} \right)^{\frac{1}{2}P_+} &= \left(\frac{x_{4,k}^-}{x_{4,k}^+} \right)^{\frac{1}{2}(\frac{1}{2}(\eta_1 + \eta_2)K_4 - \eta_1(K_1 + K_3) - \eta_2(K_5 + K_7))} \\ &\times \prod_{\substack{j=1 \\ j \neq k}}^{K_4} \frac{x_{4,k}^{+\eta_1} - x_{4,j}^{-\eta_1}}{x_{4,k}^{-\eta_2} - x_{4,j}^{+\eta_2}} \prod_{j=1}^{K_3 + K_1} \frac{x_{4,k}^{-\eta_1} - x_{3,j}}{x_{4,k}^{+\eta_1} - x_{3,j}} \prod_{j=1}^{K_5 + K_7} \frac{x_{4,k}^{-\eta_2} - x_{5,j}}{x_{4,k}^{+\eta_2} - x_{5,j}} + \mathcal{O}\left(\frac{1}{P_+^2}\right), \end{aligned} \quad (3.22)$$

Putting all $K_j = 0$, for $j \neq 4$, we indeed reproduce the results for the rank one subsectors presented in [23]. This explains the simple form of the equations established there.

4. Large P_+ expansion

We will now explicitly expand the Bethe equations in the large P_+ limit. The mode numbers of the string oscillators will enter in the equations as the zero mode of the magnon momenta p_k . However, depending on if we are looking at a state with confluent mode numbers or not, the procedure is somewhat different. We will begin with the simpler case where all mode numbers are distinct.

4.1 Non-confluent mode numbers

For distinct mode numbers one assumes an expansion of p_k as [20, 23]

$$p_k = \frac{p_k^0}{P_+} + \frac{p_k^1}{P_+^2}. \quad (4.1)$$

Determining the analogous expansion of $x_{4,k}^\pm$

$$x_{4,k}^\pm = P_+ x_{4,k}^0 + x_{4,k}^{1,\pm} + \dots, \quad (4.2)$$

where

$$x_{4,k}^0 = \frac{1 + \omega_k}{2p_k^0}, \quad x_{4,k}^{1,\pm} = \frac{1}{4}(1 + \omega_k) \left(\pm i - \frac{2p_k^1}{(p_k^0)^2 \omega_k} \right), \quad (4.3)$$

and $\omega_k = \sqrt{1 + \tilde{\lambda} \frac{(p_k^0)^2}{16\pi^2}}$. Consistency then implies that the spectral parameters $x_{3,k}$ and $x_{5,k}$ have the expansion⁵

$$x_{3,k} = P_+ x_{3,k}^0 + x_{3,k}^1 + \dots, \quad x_{5,k} = P_+ x_{5,k}^0 + x_{5,k}^1 + \dots. \quad (4.4)$$

Taking the logarithm of (3.22) and expanding we find that the momentum at leading order p_k^0 in (4.1) satisfy

$$p_k^0 = 4\pi m_k, \quad m_k \in \mathbb{Z}, \quad (4.5)$$

the integer here is what will correspond to the mode numbers of the string oscillators. Expanding (3.22) to the next order we find that the p_k^1 should satisfy

$$\begin{aligned} p_k^1 = & \frac{1}{2}(\eta_1 + \eta_2) \sum_{\substack{j=1 \\ j \neq k}}^{K_4} \frac{2 + \omega_k + \omega_j}{x_{4,k}^0 - x_{4,j}^0} - \eta_1 \sum_{j=1}^{K_1+K_3} \frac{1 + \omega_k}{x_{4,k}^0 - x_{3,j}^0} \\ & - \eta_2 \sum_{j=1}^{K_5+K_7} \frac{1 + \omega_k}{x_{4,k}^0 - x_{5,j}^0} - \left(\frac{1}{2}(\eta_1 + \eta_2)K_4 - \eta_1(K_1 + K_3) - \eta_2(K_5 + K_7) \right) p_k^0. \end{aligned} \quad (4.6)$$

⁵The expansion of $x_{3,k}$ and $x_{5,k}$ remains the same in the case of confluent mode numbers, while the expansion of $x_{4,k}^\pm$ differs.

We also want to expand the light-cone energy (3.19), using (3.18) and (3.8) we find

$$P_- = - \sum_{k=1}^{K_4} \omega_k + \delta P_-, \quad (4.7)$$

where the energy shift, δP_- , is given by

$$\delta P_- = - \frac{\tilde{\lambda}}{P_+} \frac{1}{16\pi^2} \sum_{k=1}^{K_4} \frac{p_k^0 p_k^1}{\omega_k}. \quad (4.8)$$

4.2 Confluent mode numbers

For the case of confluent mode numbers we run into trouble because of the zero denominator in (4.6), which is caused by the term

$$\prod_{\substack{j=1 \\ j \neq k}}^{K_4} \frac{x_{4,k}^{+\eta_1} - x_{4,j}^{-\eta_1}}{x_{4,k}^{-\eta_2} - x_{4,j}^{+\eta_2}} \quad (4.9)$$

of (3.22). One could try to only look at the case with the gradings chosen so that $\pm\eta_1 = \mp\eta_2$. However, this would mean that we pick a fermionic vacuum in the nested Bethe ansatz and since the rapidities $x_{4,k}$ are degenerate, we end up with zero. So for the case of confluent mode numbers we are forced to pick $\eta_1 = \eta_2$.

The way to proceed is to assume an expansion of p_k as [20],

$$p_k = \frac{p_k^0}{P_+} + \frac{p_{k,l_k}^1}{P_+^{3/2}} + \frac{p_{k,l_k}^2}{P_+^2}. \quad (4.10)$$

Where we, following [20], denote the multiplicity of the degeneracy as ν_k so $\sum_{k=1}^{K'_4} \nu_k = K_4$ and $\sum_{k=1}^{K'_4} \nu_k m_k = 0$, where K'_4 is the number of distinct mode numbers. The first order term in (4.10) is degenerate for confluent mode numbers while for the higher order terms the degeneracy might be lifted ($l_k \in \{1, 2, \dots, \nu_k\}$).

Using (4.10) the energy shift will decompose as

$$\delta P_- = \sum_{k=1}^{K'_4} \sum_{l_k=1}^{\nu_k} \delta P_{-,k,l_k}. \quad (4.11)$$

The contribution from mode numbers m_j with $\nu_j = 1$ look the same as in (4.8) while modes m_k with $\nu_k > 1$ will have contribution from p_{k,l_k}^1 . Using (4.10) and expanding (4.9) we find that p_{k,l_k}^1 satisfy a Stieltjes equation [30] of the form [20]

$$p_{k,l_k}^1 = -2(\eta_1 + \eta_2)(p_k^0)^2 \omega_k \sum_{\substack{\mu_k=1 \\ \mu_k \neq l_k}}^{\nu_k} \frac{1}{p_{k,l_k}^1 - p_{k,\mu_k}^1}. \quad (4.12)$$

It is useful to note that $\sum_{l_k=1}^{\nu_k} p_{k,l_k}^1 = 0$. The momenta p_{k,l_k}^1 can be written as

$$(p_{k,l_k}^1)^2 = -2(\eta_1 + \eta_2)(p_k^0)^2 \omega_k h_{\nu_k, l_k}^2 \quad \text{with } l_k = 1, \dots, \nu_k \quad (4.13)$$

where h_{ν_k, l_k} are the ν_k roots of Hermite polynomials of degree ν_k . However, the explicit solutions h_{ν_k, l_k} are not needed since when summing over k the following property applies

$$\sum_{l_k=1}^{\nu_k} (h_{\nu_k, l_k})^2 = \frac{\nu_k(\nu_k - 1)}{2}. \quad (4.14)$$

The expansion for the second order contribution p_{k,l_k}^2 in (4.10) is considerably more complicated, we therefore refer only to its general structure

$$p_{k,l_k}^2 = \tilde{p}_k^2 + \sum_{\substack{\mu_k=1 \\ \mu_k \neq l_k}}^{\nu_k} f_k(\mu_k, l_k). \quad (4.15)$$

We split p_{k,l_k}^2 into a part not depending on l_k , which is equivalent to p_k^1 given in (4.6): $\tilde{p}_k^2 \equiv p_k^1$. The function f_k has the property $f_k(\mu_k, l_k) = -f_k(l_k, \mu_k)$ and thus the second term drops out when summed over l_k . The final expression for the energy shift becomes then

$$\begin{aligned} \delta P_- &= -\frac{1}{P_+} \frac{\tilde{\lambda}}{16\pi^2} \sum_{k=1}^{K'_4} \sum_{l_k=1}^{\nu_k} \frac{\frac{1}{2}(p_{k,l_k}^1)^2 + p_k^0 \omega_k^2 p_{k,l_k}^2}{\omega_k^3} \\ &= -\frac{1}{P_+} \frac{\tilde{\lambda}}{32\pi^2} \sum_{k=1}^{K'_4} \nu_k p_k^0 \left(\frac{2\tilde{p}_k^2 \omega_k - (\eta_1 + \eta_2) p_k^0 (\nu_k - 1)}{\omega_k^2} \right). \end{aligned} \quad (4.16)$$

4.3 Bethe equations for the smaller spin chains

To be able to solve for p_k^1 it is clear from the form of (4.6) that we need the values of the Bethe roots $x_{3,k}$ and $x_{5,k}$ at leading order in P_+ . Note that the variables u_k scale as $u_k = P_+ u_k^0 + u_k^1 + \dots$. Expanding (3.2), (3.3), (3.5) and (3.6) yields

$$\begin{aligned} 0 &= \sum_{\substack{j=1 \\ j \neq k}}^{K_2} \frac{2}{u_{2,j}^0 - u_{2,k}^0} + \sum_{j=1}^{K_1+K_3} \frac{1}{u_{2,k}^0 - (x_{3,j}^0 + \frac{\tilde{\lambda}}{64\pi^2} \frac{1}{x_{3,j}^0})}, \\ 0 &= \eta_1 \sum_{j=1}^{K_2} \frac{1}{x_{3,k}^0 + \frac{\tilde{\lambda}}{64\pi^2} \frac{1}{x_{3,k}^0} - u_{2,j}^0} + \frac{1}{2} \sum_{j=1}^{K_4} \frac{1 + \omega_j}{x_{4,j}^0 - x_{3,k}^0}, \\ 0 &= \eta_2 \sum_{j=1}^{K_6} \frac{1}{x_{5,k}^0 + \frac{\tilde{\lambda}}{64\pi^2} \frac{1}{x_{5,k}^0} - u_{6,j}^0} + \frac{1}{2} \sum_{j=1}^{K_4} \frac{1 + \omega_j}{x_{4,j}^0 - x_{5,k}^0}, \\ 0 &= \sum_{\substack{j=1 \\ j \neq k}}^{K_6} \frac{2}{u_{6,j}^0 - u_{6,k}^0} + \sum_{j=1}^{K_5+K_7} \frac{1}{u_{6,k}^0 - (x_{5,j}^0 + \frac{\tilde{\lambda}}{64\pi^2} \frac{1}{x_{5,j}^0})}, \end{aligned} \quad (4.17)$$

which determine the $x_{2,k}^0$, $x_{3,k}^0$, $x_{5,k}^0$ and $x_{6,k}^0$ in terms of $x_{4,k}^0$. Note that the two sets of the first two and the last two equations are decoupled and identical in structure.

Let us briefly discuss how one goes about solving these equations for a given excitation sector. First one needs to commit oneself to a specific grading by specifying the numbers $\eta_{1,2} = \pm 1$. Then one reads off the values for $\{K_i\}$ in table 1 corresponding to the excitation pattern in question. The four different choices of gradings can be grouped into two classes, one with fermionic middle node, $\eta_1 = -\eta_2$, and one with bosonic middle node, $\eta_1 = \eta_2$ in the associated Dynkin diagram. The difference between the two is important in the case of confluent mode numbers. The K_3 and K_5 (and for $\eta_1 = -\eta_2$, also K_4) are fermionic nodes which means that the solutions for $x_{3,k}^0$ and similarly for $x_{5,k}^0$ for different values of k are not allowed to be degenerate by the Pauli principle.

Consider for example the $\mathfrak{su}(1, 1|2)$ sector containing only nonvanishing values for $\{K_3, K_4, K_5\}$. Then, due to $K_2 = 0 = K_6$, the equations (4.17) condense to two identical, degree K_4 polynomial equations for $x_{3,k}^0$ and $x_{5,k}^0$ yielding K_4 solutions, including the degenerate solution $\{x_{3/5,k}^0 \rightarrow \infty\}$. These K_4 solutions are then used once on each node K_3 and K_5 , each generating $\frac{K_4(K_4-1)\times\dots\times(K_4-K_j)}{K_j!}$ (with $j = 3, 5$) number of solutions. For a bosonic node, however, we may pick the same solution repeatedly.

Having distributed the solutions for $x_{3,k}^0$ and $x_{5,k}^0$ one then determines p_k^1 from (4.6) and finally solves for the energy shift using (4.8) or (4.16). The obtained value is what we then compare with a direct diagonalization of the string Hamiltonian.

5. Comparing the Bethe equations with string theory

We have calculated the energy shifts (both analytically and numerically) for a large number of states. The numerical results will be presented in appendix B, while here in the main text we shall focus on the analytical results. On the string theory side one studies the Hamiltonian in first order degenerate perturbation theory, which in practice demands the diagonalization of the Hamiltonian in the relevant subsectors. In the near plane-wave limit, this was first done by Callan, McLoughlin, Swanson and coworkers in [17] using a different gauge.

5.1 General structure of solutions

We will present analytical results for three different sectors, $\mathfrak{su}(1|2)$, $\mathfrak{su}(1, 1|2)$ and $\mathfrak{su}(2|3)$. The operators in each sector are

$$\mathfrak{su}(1|2) : \quad \{\alpha_1^+, \theta_1^+\}, \quad \mathfrak{su}(1, 1|2) : \quad \{\alpha_1^+, \beta_1^+, \theta_1^+, \eta_1^+\}, \quad \mathfrak{su}(2|3) : \quad \{\alpha_1^+, \alpha_2^+, \theta_1^+, \theta_2^+\}.$$

As we can see there is a mixing between the sectors, the $\mathfrak{su}(1|2)$ is contained within the larger $\mathfrak{su}(2|3)$ sector and in $\mathfrak{su}(1, 1|2)$, but the latter is not a part of $\mathfrak{su}(2|3)$. When

calculating the energy shifts, things are straightforward for the first two sectors, $\mathfrak{su}(1|2)$ and $\mathfrak{su}(1, 1|2)$. The excited nodes are K_3 , K_4 and K_5 and for these excitation numbers (4.17) is significantly simplified since there are no $u_{2,k}$ roots. Each $x_{3,k}$ and $x_{5,k}$ satisfy a $K_2 - \nu$ degree polynomial equation, where ν is the number of confluent mode numbers, which is the same for each value of k . However, this is not the case for the $\mathfrak{su}(2|3)$ sector where we have nonvanishing K_2 excitations and a resulting set of coupled polynomial equations for the $x_{2,k}$ and $x_{3,k}$ following from (4.17)

5.2 The $\mathfrak{su}(1|2)$ sector

As stated, this sector is spanned by the oscillators α_1^+ and θ_1^+ . The contributing parts from the string Hamiltonian are \mathcal{H}_{bb} and \mathcal{H}_{bf} . The explicit expression for the effective $\mathfrak{su}(1|2)$ Hamiltonian can be found in (A.8). Let us count the number of solutions for the grading $\eta_1 = \eta_2 = 1$. Then the only excited nodes of the Dynkin diagram in this sector are K_4 and K_3 , so the polynomials in (4.17) give $K_4 - \nu$ solutions⁶. Two of these solutions are always 0 and ∞ while the other $K_4 - 2 - \nu$ are non-trivial. Before we perform the actual computation let us count the number of solutions. Say we have a total of K_3 θ_1^+ oscillators and $K_4 - K_3$ α_1^+ oscillators, then this state will yield $\frac{(K_4 - \nu) \times (K_4 - \nu - 1) \times \dots \times (K_4 - \nu - K_3 + 1)}{K_3!}$ number of solutions. So, for all possible combinations of a general K_4 impurity state the number of solutions are

$$\sum_{K_3=0}^{K_4-\nu} \binom{K_4 - \nu}{K_3} = 2^{K_4 - \nu}. \quad (5.1)$$

Since the worldsheet Hamiltonian is a $2^{K_4 - \nu} \times 2^{K_4 - \nu}$ matrix, the number of solutions matches.

5.2.1 Two impurities

For the two impurity sector the perturbative string Hamiltonian is a 4×4 matrix, but we are only interested in a 2×2 submatrix since the other part falls into the rank one sectors $\mathfrak{su}(2)$ and $\mathfrak{su}(1|1)$. The relevant matrix elements, with mode numbers $\{q, -q\}$, are

$$\left(\begin{array}{c|cc} & |\alpha_{1,q}^+ \theta_{1,-q}^+ |0\rangle & |\alpha_{1,-q}^+ \theta_{1,q}^+ |0\rangle \\ \hline \langle 0 | \alpha_{1,q}^- \theta_{1,-q}^- & \mathcal{H}_{bf} & \mathcal{H}_{bf} \\ \hline \langle 0 | \alpha_{1,-q}^- \theta_{1,q}^- & \mathcal{H}_{bf} & \mathcal{H}_{bf} \end{array} \right)$$

The energy shifts are the non-zero values in (A.10). Now, the interesting question is of course if we can reproduce this result from the Bethe equations. For the two impurity state $\alpha^+ \theta^+ |0\rangle$ it is easiest to work with the gradings⁷ $\eta_1 = -1$ and $\eta_2 = 1$

⁶The number of confluent mode numbers must satisfy, $\nu \leq K_4 - K_3 + 1$ since we cannot have fermionic excitations of the same flavor with confluent mode numbers.

⁷All choices of gradings of course give the same result, however, the calculation will be more or less complicated depending on the choice.

where we have $K_4 = 2$ and $K_3 = 1$. From (4.17) we see that the only solutions for $x_{3,k}$ are 0 and ∞ . Since we have two roots, and one K_3 excitation we get two solutions for p_k^1 . Solving (4.6) gives $p_k^1 = \pm p_k^0$. Plugging these into (4.8) gives

$$\delta P_- = \pm \frac{\tilde{\lambda}}{P_+} \sum_{j=1}^2 \frac{q_j^2}{\omega_{q_j}} = \pm 2 \frac{\tilde{\lambda}}{P_+} \frac{q^2}{\omega_q} =: \kappa_2, \quad (5.2)$$

which equals the non-zero values in (A.10).

5.2.2 Three impurities, distinct mode numbers

The full perturbative string Hamiltonian is a 8×8 matrix but the relevant $\mathfrak{su}(1|2)$ part splits up into two independent submatrices coming from the Fermi-Fermi matrix elements $\langle 0 | \alpha_1^- \alpha_1^- \theta_1^- (\mathcal{H}_{bb} + \mathcal{H}_{bf}) \theta_1^+ \alpha_1^+ \alpha_1^+ | 0 \rangle$ and the Bose-Bose elements $\langle 0 | \alpha_1^- \theta_1^- \theta_1^- (\mathcal{H}_{bf}) \theta_1^+ \theta_1^+ \alpha_1^+ | 0 \rangle$. Schematically written we have,

$$\left(\begin{array}{c|c|c} & \alpha_1^+ \alpha_1^+ \theta_1^+ | 0 \rangle & \alpha_1^+ \theta_1^+ \theta_1^+ | 0 \rangle \\ \hline \langle 0 | \theta_1^- \alpha_1^- \alpha_1^- & (\mathcal{H}_{bb} + \mathcal{H}_{bf})^{3 \times 3} & 0_{3 \times 3} \\ \hline \langle 0 | \theta_1^- \theta_1^- \alpha_1^- & 0_{3 \times 3} & \mathcal{H}_{bf}^{3 \times 3} \end{array} \right) \quad (5.3)$$

The eigenvalues of the Bose-Bose submatrix, the bottom right, is given in (A.11). To reproduce these shifts from the Bethe equations we once again choose $\eta_1 = -1$ and $\eta_2 = 1$ so $K_4 = 3$ and $K_3 = 1$. Solving (4.17) give, as before, $x_{3,k}^0 = \{0, \infty\}$ together with a novel third solution

$$y = \frac{(2 + \omega_{q_1} + \omega_{q_2}) x_{4,3}^0 + (2 + \omega_{q_2} + \omega_{q_3}) x_{4,1}^0 + (2 + \omega_{q_1} + \omega_{q_3}) x_{4,2}^0}{3 + \omega_{q_1} + \omega_{q_2} + \omega_{q_3}}. \quad (5.4)$$

The first two solutions, 0 and ∞ , give as before $p_k^1 = \pm p_k^0$. For generic values of K_4 , and with $K_3 = 1$, these two solutions will always appear. Using the third solution in (4.6) yields

$$p_k^1 = \frac{1 + \omega_k}{x_{4,k}^0 - y} - p_k^0. \quad (5.5)$$

Plugging this into (4.8), together with some algebra, gives the three solutions

$$\delta P_- = \left\{ \pm \frac{\tilde{\lambda}}{P_+} \sum_{j=1}^3 \frac{q_j^2}{\omega_{q_j}}, \frac{\tilde{\lambda}}{P_+ \omega_{q_1} \omega_{q_2} \omega_{q_3}} \sum_{j=1}^3 q_j^2 \omega_{q_j} \right\} =: \Lambda_3, \quad (5.6)$$

which agrees with the string result obtained in (A.11).

Let us now focus on the Fermi-Fermi matrix elements, the upper left 3×3 block of (5.3). First, (4.17) give the same three solutions as before, namely $\{0, \infty, y\}$ with

the same y as in (5.4). Since $K_3 = 2$ we now, for each p_k^1 , use two of the solutions for $x_{3,k}^0$

$$p_k^1 = (1 + \omega_{p_k^0}) \left(\frac{1}{x_{4,k}^0 - x_{3,1}^0} + \frac{1}{x_{4,k}^0 - x_{3,2}^0} \right) - 2p_k^0. \quad (5.7)$$

The three possible distributions of the roots, $\{0, \infty\}$, $\{0, y\}$ and $\{y, \infty\}$, give the three solutions

$$\delta P_- = \left\{ 0, -\frac{\tilde{\lambda}}{P_+} \frac{1}{16\pi^2} \sum_{j=1}^{K_4} \frac{p_k^0}{\omega_k} \left(\left(\frac{1 + \omega_k}{x_{4,k}^0 - y} - p_k^0 \right) \pm p_k^0 \right) \right\} =: \Omega_3 \quad (5.8)$$

With a little bit of work one can show that these match the eigenvalues from the string Hamiltonian in (A.12).

5.2.3 Three impurities, confluent mode numbers

For three impurities, with mode numbers $\{q, q, -2q\}$, the only state that does not fall into the already checked rank one sectors [23] are $\alpha_1^+ \alpha_1^+ \theta_1^+ |0\rangle$ and $\alpha_1^+ \theta_1^+ \theta_1^+ |0\rangle$. For the former, we get from (4.6) (with grading $\eta_1 = \eta_2 = 1$)

$$\tilde{p}_q^2 = -2p_q^0 + \frac{2\omega_q + \omega_{2q}}{x_{4,q}^0 - x_{4,2q}^0} - \frac{1 + \omega_q}{x_{4,q}^0 - x_3^0}, \quad \tilde{p}_{2q}^2 = -2p_{2q}^0 + 2\frac{2\omega_q + \omega_{2q}}{x_{4,2q}^0 - x_{4,q}^0} - \frac{1 + \omega_{2q}}{x_{4,2q}^0 - x_3^0}.$$

The polynomials in (4.17) give two solutions $\{0, \infty\}$ for $x_{3,k}^0$. Using these in (4.16), together with some algebra, gives

$$\delta P_- = \frac{2q^2 \tilde{\lambda}}{P_+ \omega_q^2 \omega_{2q}} \left\{ \frac{3\omega_{2q} + (2\omega_q + \omega_{2q})(4\omega_q(1 + \omega_q) + \omega_{2q})}{3 + 2\omega_q + \omega_{2q}}, \right. \\ \left. - \frac{4\omega_q^2 - (3 - 4\omega_q^2)\omega_{2q} - (1 - 2\omega_q)\omega_{2q}^2}{3 + 2\omega_q + \omega_{2q}} \right\}. \quad (5.9)$$

It is not immediately apparent that this equals the string Hamiltonian result (A.14) but after some work one can show that these two solutions are equal.

For the second state, $\alpha_1^+ \theta_1^+ \theta_1^+ |0\rangle$, we have $K_3 = 2$ and the two roots $\{0, \infty\}$ for $x_{3,k}^0$ can only be distributed in one way. By doing analogously as above and using (4.6) in (4.16), we find

$$\delta P_- = \frac{2q^2 \tilde{\lambda}}{P_+} \frac{(\omega_q + \omega_{2q})}{\omega_q \omega_{2q}}, \quad (5.10)$$

which reproduces the string Hamiltonian result of (A.13).

5.3 The $\mathfrak{su}(1, 1|2)$ sector

Now we turn to the larger $\mathfrak{su}(1, 1|2)$ sector. The procedure is the same as above but now both sides of the Dynkin diagram gets excited and a general state has the three middle nodes K_3, K_4 and K_5 excited. We are allowed to pick the same solution, on the K_3 and K_5 node, but as before we must put distinct solutions on the fermionic nodes. In this sector a new feature appears: The states $\alpha_1^+ \beta_1^+$ and $\theta_1^+ \eta_1^+$ are allowed to mix. Also, in the case of confluent mode numbers, it turns out that we have to make use of different gradings on some states to generate all the solutions from the string Hamiltonian.

Let us first investigate if the number of solutions from the string Hamiltonian and the Bethe equations match. A general $\mathfrak{su}(1, 1|2)$ state with K_4 excitations and *distinct* mode numbers will yield a $2^{2K_4} \times 2^{2K_4}$ matrix and thus 2^{2K_4} energy shifts. The total number of solutions from the Bethe equations are just the square of (5.1), with $\nu = 0$, which equals the number of eigenvalues from the perturbative string Hamiltonian (A.15).

5.3.1 Two impurities

The Hamiltonian is a 16×16 matrix but it is only a 13×13 part which lies outside the already calculated $\mathfrak{su}(1|2)$ sector. There are seven different independent submatrices where the largest is a 4×4 matrix and is generated by the base kets $\alpha_1^+ \beta_1^+ |0\rangle$ and $\theta_1^+ \eta_1^+ |0\rangle$. There are three 2×2 submatrices, $\alpha_1^+ \eta_1^+ |0\rangle, \beta_1^+ \theta_1^+ |0\rangle$ and $\beta_1^+ \eta_1^+ |0\rangle$. And three are one valued $\beta_1^+ \beta_1^+ |0\rangle, \eta_1^+ \eta_1^+ |0\rangle$ and $\theta_1^+ \theta_1^+ |0\rangle$, these will give the same results as presented in [23] so these we will ignore. The only part with mixing is the subpart generated by $\alpha_1^+ \beta_1^+ |0\rangle$ and $\theta_1^+ \eta_1^+ |0\rangle$. To calculate the energy shifts we start by solving (4.17) and, as before, the two solutions are $\{0, \infty\}$. With $\eta_1 = -1$ and $\eta_2 = 1$, so $K_4 = 3$ and $K_5 = K_3 = 1$, we have

$$p_k^1 = (1 + \omega_k) \left(\frac{1}{x_{4,k}^0 - x_{3,k}^0} - \frac{1}{x_{4,k}^0 - x_{5,k}^0} \right). \quad (5.11)$$

Whenever we pick the same solution for $x_{3,k}^0$ and $x_{5,k}^0$ we get zero and since we can do this in two ways we get two zero solutions. The other two solutions are obtained by setting $\{x_{3,k}^0, x_{5,k}^0\} = \{0, \infty\}$ and $\{\infty, 0\}$ which gives $p_k^1 = \pm 2p_k^0$. Using this in (4.8) gives

$$\delta P_- = (0, 0, \pm \frac{2\tilde{\lambda}}{P_+} \sum_{j=1}^2 \frac{q_j^2}{\omega_{q_j}}), \quad (5.12)$$

which is in agreement with the string Hamiltonian result in (A.16).

For the three parts $\alpha^+ \eta^+ |0\rangle, \beta^+ \theta^+ |0\rangle$ and $\beta^+ \eta^+ |0\rangle$, we see that solving for the first state is analogous to the discussion after (5.2) but with $\eta_1 = 1$ and $\eta_2 = -1$. For the two other, the procedure will again be identical if we choose the opposite

$\{\eta_1, \eta_2\}$	$\{K_1 + K_3, K_4, K_5 + K_7\}$	$\{S_+, S_-, J_+, J_-\}$	δP_-
$\{-, +\}$	$\{2, 3, 0\}$	$\{0, 1, 3, 2\}_{\alpha_1^+ \alpha_1^+ \theta_1^+}$	Ω_3
$\{+, -\}$	$\{0, 3, 2\}$	$\{1, 0, 2, 3\}_{\alpha_1^+ \alpha_1^+ \eta_1^+}$	$-\Omega_3$
$\{-, +\}$	$\{0, 3, 2\}$	$\{2, 3, 1, 0\}_{\beta_1^+ \beta_1^+ \theta_1^+}$	Ω_3
$\{+, -\}$	$\{2, 3, 0\}$	$\{3, 2, 0, 1\}_{\beta_1^+ \beta_1^+ \eta_1^+}$	$-\Omega_3$
$\{-, +\}$	$\{1, 3, 0\}$	$\{0, 2, 3, 1\}_{\theta_1^+ \theta_1^+ \alpha_1^+}$	Λ_3
$\{-, +\}$	$\{0, 3, 1\}$	$\{1, 3, 2, 0\}_{\theta_1^+ \theta_1^+ \beta_1^+}$	$-\Lambda_3$
$\{+, -\}$	$\{0, 3, 1\}$	$\{2, 0, 1, 3\}_{\eta_1^+ \eta_1^+ \alpha_1^+}$	Λ_3
$\{+, -\}$	$\{1, 3, 0\}$	$\{3, 1, 0, 2\}_{\eta_1^+ \eta_1^+ \beta_1^+}$	$-\Lambda_3$

Table 2: The states reproducing the 3×3 submatrices of the string Hamiltonian. Ω_3 and Λ_3 , where the subscript indicate the number of solutions as given in (5.8) for Ω_3 and (5.6) for Λ_3 .

$\{\eta_1, \eta_2\}$	$\{K_1 + K_3, K_4, K_5 + K_7\}$	$\{S_+, S_-, J_+, J_-\}$	δP_-
$\{+, +\}$	$\{1, 3, 1\}$	$\{1, 1, 2, 2\}_{(\alpha_1^+ \alpha_1^+ \beta_1^+), (\alpha_1^+ \theta_1^+ \eta_1^+)}$	Ω_9
$\{-, -\}$	$\{1, 3, 1\}$	$\{2, 2, 1, 1\}_{(\alpha_1^+ \beta_1^+ \beta_1^+), (\beta_1^+ \theta_1^+ \eta_1^+)}$	$-\Omega_9$
$\{-, +\}$	$\{1, 3, 1\}$	$\{1, 2, 2, 1\}_{(\alpha_1^+ \beta_1^+ \theta_1^+), (\theta_1^+ \theta_1^+ \eta_1^+)}$	Λ_9
$\{+, -\}$	$\{1, 3, 1\}$	$\{2, 1, 1, 2\}_{(\alpha_1^+ \beta_1^+ \eta_1^+), (\theta_1^+ \eta_1^+ \eta_1^+)}$	$-\Lambda_9$

Table 3: The states reproducing the 9×9 submatrices of the string Hamiltonian. Ω_9 and Λ_9 , where the subscript indicate the number of solutions, is given by (5.14) and (5.15).

gradings. That is, for $\beta^+ \theta^+ |0\rangle$ we pick $\eta_1 = 1$ and $\eta_2 = -1$, while for $\beta^+ \eta^+ |0\rangle$ we choose $\eta_1 = -1$ and $\eta_2 = 1$ which give the same set of solution for all three states

$$\delta P_- = \pm \frac{2\tilde{\lambda} q^2}{P_+ \omega_q}, \quad (5.13)$$

which is in agreement with (A.17).

5.3.2 Three impurities, distinct mode numbers

The full perturbative string Hamiltonian will now be a 64×64 matrix with non trivial 3×3 and 9×9 subsectors. Since the logic of solving the Bethe equation should be clear by now, we only present the obtained results in tabular form. Also, to make the comparison with the string Hamiltonian more transparent, we now also label the states by their charges $\{S_+, S_-, J_+, J_-\}$. The energy shifts for the 3×3 parts are given in table 2 and for the larger 9×9 subparts in table 3. For the larger sectors we have a mixing between states of different boson and fermion number.

$\{\eta_1, \eta_2\}$	$\{K_1 + K_3, K_4, K_5 + K_7\}$	$\{S_+, S_-, J_+, J_-\}$	δP_-
$\{+, +\}$	$\{1, 3, 0\}$	$\{0, 1, 3, 2\}_{\alpha_1^+ \alpha_1^+ \theta_1^+}$	$\tilde{\Omega}_2$
$\{+, +\}$	$\{0, 3, 1\}$	$\{1, 0, 2, 3\}_{\alpha_1^+ \alpha_1^+ \eta_1^+}$	$\tilde{\Omega}_2$
$\{-, -\}$	$\{0, 3, 1\}$	$\{2, 3, 1, 0\}_{\beta_1^+ \beta_1^+ \theta_1^+}$	$-\tilde{\Omega}_2$
$\{-, -\}$	$\{1, 3, 0\}$	$\{3, 2, 0, 1\}_{\beta_1^+ \beta_1^+ \eta_1^+}$	$-\tilde{\Omega}_2$
$\{+, +\}$	$\{2, 3, 0\}$	$\{0, 2, 3, 1\}_{\theta_1^+ \theta_1^+ \alpha_1^+}$	$\tilde{\Lambda}_1$
$\{-, -\}$	$\{0, 3, 2\}$	$\{1, 3, 2, 0\}_{\theta_1^+ \theta_1^+ \beta_1^+}$	$-\tilde{\Lambda}_1$
$\{+, +\}$	$\{0, 3, 2\}$	$\{2, 0, 1, 3\}_{\eta_1^+ \eta_1^+ \alpha_1^+}$	$\tilde{\Lambda}_1$
$\{-, -\}$	$\{2, 3, 0\}$	$\{3, 1, 0, 2\}_{\eta_1^+ \eta_1^+ \beta_1^+}$	$-\tilde{\Lambda}_1$

Table 4: The states reproducing the 2×2 submatrices for *confluent* mode numbers of the string Hamiltonian. $\tilde{\Omega}_2$ and $\tilde{\Lambda}_2$, where the subscript indicate the number of solutions, is given by (5.9) and (5.10)

The functions Ω_9 and Λ_9 in table 3 depend on the mode numbers $\{q_1, q_2, q_3\}$ and are given by

$$\Omega_9 = \frac{\tilde{\lambda}}{P_+} \frac{1}{16\pi^2} \sum_{k=1}^3 \frac{p_{q_k}^0}{\omega_{q_k}} \left(\sum_{j=1, j \neq k}^3 \frac{2 + \omega_{q_k} + \omega_{q_j}}{x_{4,q_k}^0 - x_{4,q_j}^0} - \frac{1 + \omega_{q_k}}{x_{4,q_k}^0 - x_3^0} - \frac{1 + \omega_{q_k}}{x_{4,q_k}^0 - x_5^0} \right) - p_{q_k}^0 \quad (5.14)$$

$$\Lambda_9 = -\frac{\tilde{\lambda}}{P_+} \frac{1}{16\pi^2} \sum_{k=1}^3 \frac{p_{q_k}^0}{\omega_{q_k}} \left(\frac{1 + \omega_{q_k}}{x_{4,q_k}^0 - x_3^0} - \frac{1 + \omega_{q_k}}{x_{4,q_k}^0 - x_5^0} \right). \quad (5.15)$$

To obtain the nine solutions for Ω_9 and Λ_9 one has to insert one of the three roots $\{0, \infty, y\}$ for each x_3^0 and x_5^0 . We have not managed to match these results with the perturbative string Hamiltonian (A.15) analytically, but tested the agreement extensively numerically. The details of the numerical tests can be found in Appendix B.

5.3.3 Three impurities, confluent mode numbers

We will now look at three impurities with confluent mode numbers, $\{q, q, -2q\}$. With two distinct mode numbers we see from (4.17) that we have the two standard solutions $\{0, \infty\}$ for $x_{3,k}^0$ and $x_{5,k}^0$. The sectors exhibiting mixing, i.e. the states that span the 9×9 subparts of the previous section, now exhibit a new feature. The gradings are no longer equivalent and we will be forced to use both to generate all the desired solutions. The simpler states, that do not exhibit this feature, are presented in table 4 and the states where different gradings had to be used are presented in table 5. The energy shifts Γ_4 and $\tilde{\Gamma}_1$ appearing in table 5 are given by

$\{\eta_1, \eta_2\}$	$\{K_1 + K_3, K_4, K_5 + K_7\}$	$\{S_+, S_-, J_+, J_-\}$	δP_-
$\{+, +\}$	$\{1, 3, 1\}$	$\{1, 1, 2, 2\}_{(\alpha_1^+ \alpha_1^+ \beta_1^+), (\alpha_1^+ \theta_1^+ \eta_1^+)}$	Γ_4
$\{-, -\}$	$\{2, 3, 2\}$	$\{1, 1, 2, 2\}_{(\alpha_1^+ \alpha_1^+ \beta_1^+), (\alpha_1^+ \theta_1^+ \eta_1^+)}$	$\tilde{\Gamma}_1$
$\{-, -\}$	$\{1, 3, 1\}$	$\{2, 2, 1, 1\}_{(\alpha_1^+ \beta_1^+ \beta_1^+), (\beta_1^+ \theta_1^+ \eta_1^+)}$	$-\Gamma_4$
$\{+, +\}$	$\{2, 3, 2\}$	$\{2, 2, 1, 1\}_{(\alpha_1^+ \beta_1^+ \beta_1^+), (\beta_1^+ \theta_1^+ \eta_1^+)}$	$-\tilde{\Gamma}_1$
$\{+, +\}$	$\{2, 3, 1\}$	$\{1, 2, 2, 1\}_{(\alpha_1^+ \beta_1^+ \theta_1^+), (\theta_1^+ \theta_1^+ \eta_1^+)}$	$\tilde{\Omega}_2$
$\{-, -\}$	$\{1, 3, 2\}$	$\{1, 2, 2, 1\}_{(\alpha_1^+ \beta_1^+ \theta_1^+), (\theta_1^+ \theta_1^+ \eta_1^+)}$	$-\tilde{\Omega}_2$
$\{-, -\}$	$\{2, 3, 1\}$	$\{2, 1, 1, 2\}_{(\alpha_1^+ \beta_1^+ \eta_1^+), (\theta_1^+ \eta_1^+ \eta_1^+)}$	$-\tilde{\Omega}_2$
$\{+, +\}$	$\{1, 3, 2\}$	$\{2, 1, 1, 2\}_{(\alpha_1^+ \beta_1^+ \eta_1^+), (\theta_1^+ \eta_1^+ \eta_1^+)}$	$\tilde{\Omega}_2$

Table 5: The states reproducing the larger submatrices, with *confluent* mode numbers, of the string Hamiltonian. The functions Γ_4 and $\tilde{\Gamma}_1$ are given in (5.16) and $\tilde{\Omega}_2$ is given in (5.9).

$\{S_+, S_-, J_+, J_-\}$	State pattern	Number of solutions
$\{2, 2, 2, 2\}$	$\theta_1^+ \theta_1^+ \eta_1^+ \eta_1^+ 0\rangle, \theta_1^+ \eta_1^+ \beta_1^+ \alpha_1^+ 0\rangle, \beta_1^+ \beta_1^+ \alpha_1^+ \alpha_1^+ 0\rangle$	36 energy shifts
$\{2, 2, 3, 3\}$	$\theta_1^+ \theta_1^+ \eta_1^+ \eta_1^+ \alpha_1^+ 0\rangle, \theta_1^+ \eta_1^+ \beta_1^+ \alpha_1^+ \alpha_1^+ 0\rangle, \beta_1^+ \beta_1^+ \alpha_1^+ \alpha_1^+ \alpha_1^+ 0\rangle$	100 energy shifts

Table 6: Checked 4 and 5 impurity states of $\mathfrak{su}(1,1|2)$.

$$\begin{aligned}
\tilde{\Gamma}_1 &= \frac{2q^2 \tilde{\lambda}}{P_+ \omega_q^2 \omega_{2q}} \left(\frac{1}{\omega_q} + \frac{1}{\omega_{2q}} \right), \\
\Gamma_4 &= -\frac{2q^2 \tilde{\lambda}}{P_+ \omega_q^2 \omega_{2q}} \left\{ \left(\frac{1}{\omega_q} + \frac{1}{\omega_{2q}} \right), \left(\frac{1}{\omega_q} + \frac{1}{\omega_{2q}} \right), \frac{3\omega_{2q} + (2\omega_q + \omega_{2q})(\omega_{2q} + \omega_q(7 + 6\omega_q + \omega_{2q}))}{3 + 2\omega_q + \omega_{2q}}, \right. \\
&\quad \left. \frac{3\omega_{2q} - (2\omega_q + \omega_{2q})(\omega_q(5 + 2\omega_q + 3\omega_{2q}) - \omega_{2q})}{3 + 2\omega_q + \omega_{2q}} \right\}. \tag{5.16}
\end{aligned}$$

Again, for the comparison to the eigenvalues of the string Hamiltonian in this sub-sector we had to resort to numerical verifications, see Appendix B for details.

5.3.4 Higher impurities

In going beyond three impurities numerical calculations on both sides, the Bethe equations and the string Hamiltonian, have been performed for a number of four and five impurity states. All numerical energy shifts match precisely, the tested configurations are listed in table 6.

5.4 The $\mathfrak{su}(2|3)$ sector

Now things become more complex. The polynomials (4.17) for a general state are highly non-linear, coupled and involve several variables. For this reason we will not be as thorough in our testing for the higher impurity cases as in the previous sections. The oscillators in this sector are $\alpha_1^+, \alpha_2^+, \theta_1^+$ and θ_2^+ where there is a mixing between $\alpha_1^+ \alpha_2^+ |0\rangle$ and $\theta_1^+ \theta_2^+ |0\rangle$. The string Hamiltonian is given in (A.18).

5.4.1 Two impurities

The $\mathfrak{su}(2|3)$ two impurity sector of the perturbative string Hamiltonian (A.18) will be a 12×12 matrix. Let us begin with the largest subpart, the one with mixing between $\alpha_1^+ \alpha_2^+ |0\rangle$ and $\theta_1^+ \theta_2^+ |0\rangle$. The excitation numbers, with grading $\eta_1 = \eta_2 = 1$, for $\alpha_1^+ \alpha_2^+ |0\rangle$ are $K_1 = K_2 = K_3 = 1$ and $K_4 = 2$ while for $\theta_1^+ \theta_2^+ |0\rangle$ we have $K_2 = 1$ and $K_3 = K_4 = 2$. Here the dynamically transformed version of the Bethe equations is advantageous, as it makes explicit that the relevant combination $K_1 + K_3 = 2$ is the same for these two states. This is how the Bethe equations take care of the mixing. Solving for u_2^0 in (4.17), and using $u_{3,k}^0 = x_{3,k}^0 + \frac{\tilde{\lambda}}{64\pi^2} \frac{1}{x_{3,k}^0}$, gives

$$u_2^0 = \frac{1}{2} \left(x_{3,1}^0 + x_{3,2}^0 + \frac{\tilde{\lambda}}{64\pi^2} \left(\frac{1}{x_{3,1}^0} + \frac{1}{x_{3,2}^0} \right) \right).$$

Plugging this into the second line of (4.17) gives

$$\begin{aligned} \frac{1}{x_{3,1}^0 - x_{3,2}^0 + \frac{\tilde{\lambda}}{64\pi^2} \left(\frac{1}{x_{3,1}^0} - \frac{1}{x_{3,2}^0} \right)} + \sum_{j=1}^2 \frac{1 + \omega_j}{x_{4,j}^0 - x_{3,1}^0} &= 0, \\ \frac{1}{x_{3,2}^0 - x_{3,1}^0 + \frac{\tilde{\lambda}}{64\pi^2} \left(\frac{1}{x_{3,2}^0} - \frac{1}{x_{3,1}^0} \right)} + \sum_{j=1}^2 \frac{1 + \omega_j}{x_{4,j}^0 - x_{3,2}^0} &= 0. \end{aligned} \quad (5.17)$$

We can add these two equations above and see that four solutions are $(x_{3,1}^0, x_{3,2}^0) = (0, 0), (0, \infty), (\infty, 0)$ and (∞, ∞) . This may at first glance seem strange since the seemingly equivalent state $\theta_1^+ \theta_2^+ |0\rangle$ only has the K_2 and K_3 node excited, implying that we can not pick the same solution twice for $x_{3,k}^0$ since K_3 is fermionic. However, the correct state to use is the $\alpha_1^+ \alpha_2^+ |0\rangle$ state. Here two different fermionic nodes K_1 and K_3 are excited and because of this we can use the same solutions on both nodes simultaneously.

Let us now turn to the calculation of the energy shifts for these four states. We use the solutions from (5.17) in (4.6) and plug this into (4.8) which gives

$$\delta P_- = \left\{ 0, 0, \pm \frac{\tilde{\lambda}}{P_+} \frac{4q^2}{\omega_q} \right\} =: \chi_4, \quad (5.18)$$

which is in perfect agreement with (A.19). The energy shifts for the other states follows immediately and we present the results in table 7. From this table we see that all the energy shifts from (A.18), presented in (A.20) and (A.19), are reproduced.

5.4.2 Higher impurities

Due to the non linearity of the polynomials relating the Bethe roots we will only present results for excitations with $K_2 = K_3 = 1$, corresponding to states of the form

$\{\eta_1, \eta_2\}$	$\{K_1 + K_3, K_2, K_4\}$	$\{S_+, S_-, J_+, J_-\}$	δP_-
$\{+, +\}$	$\{2, 1, 2\}$	$\{0, 0, 2, 0\}_{(\alpha_1^+ \alpha_2^+), (\theta_1^+ \theta_2^+)}$	χ_4
$\{-, +\}$	$\{1, 0, 2\}$	$\{0, 1, 2, 1\}_{\alpha_1^+ \theta_1^+}$	κ_2
$\{-, +\}$	$\{1, 0, 2\}$	$\{0, -1, 2, -1\}_{\alpha_2^+ \theta_2^+}$	κ_2
$\{+, +\}$	$\{1, 1, 2\}$	$\{0, -1, 2, 1\}_{\alpha_1^+ \theta_2^+}$	κ_2
$\{+, +\}$	$\{1, 1, 2\}$	$\{0, 1, 2, -1\}_{\alpha_2^+ \theta_1^+}$	κ_2

Table 7: The two impurity states that fall into to the rank ≥ 1 sectors for $\mathfrak{su}(2|3)$. Here χ_4 is given by (5.18) and κ_2 is given by (5.2). For two of the states we have permuted the space-time indices.

$\{\eta_1, \eta_2\}$	$\{K_1 + K_3, K_2, K_4\}$	$\{S_+, S_-, J_+, J_-\}$	δP_-
$\{+, +\}$	$\{1, 1, K_4\}$	$\{0, -1, K_4, K_4 - 1\}_{(\alpha_1^+ \dots \alpha_1^+ \theta_2^+)}$	Λ_{K_4}

Table 8: Higher impurity states from the $\mathfrak{su}(2|3)$ sector for states of the form $\alpha_1^+ \dots \alpha_1^+ \theta_2^+ |0\rangle$. The function Λ_{K_4} , where K_4 indicates the number of solutions, is given in (5.20).

$\alpha_1^+ \dots \alpha_1^+ \theta_2^+ |0\rangle$ with space-time charge vector $\{S_+, S_-, J_+, J_-\} = \{0, -1, K_4, K_4 - 1\}$. From the first line in (4.17) we see that

$$\frac{1}{u_2^0 - (x_3^0 + \frac{\tilde{\lambda}}{64\pi^2} \frac{1}{x_3^0})} = 0,$$

and using this in the second line implies that the equation for x_3^0 reduces to the familiar form

$$\sum_{j=1}^{K_4} \frac{1 + \omega_j}{x_{4,j}^0 - x_3^0} = 0. \quad (5.19)$$

Thus, the energy shift for this state is the same as for the $\alpha_1^+ \dots \alpha_1^+ \theta_1^+ |0\rangle$ states. For $K_4 = 3$, the energy shift is presented in (5.6). For $K_4 - 1$ number of α_1^+ excitations and one θ_2^+ excitation, the energy shift, with gradings $\{+, +\}$, is given by

$$\Lambda_{K_4} = \frac{1}{16\pi^2} \sum_{k=1}^{K_4} \frac{p_k^0}{\omega_k} \left(\sum_{\substack{j=1 \\ j \neq k}}^{K_4} \frac{2 + \omega_j + \omega_k}{x_{4,k}^0 - x_{4,j}^0} - \frac{1 + \omega_k}{x_{4,k}^0 - x_3^0} - p_k^0 (K_4 - 1) \right). \quad (5.20)$$

This prediction we have verified numerically for $K_4 \leq 6$ with the energy shifts obtained by diagonalization of the string Hamiltonian (A.18).

6. Summary

In this work we have explored the quantum integrability of the $AdS_5 \times S^5$ superstring by confronting the conjectured set of Bethe equations with an explicit diagonalization of the light-cone gauged string Hamiltonian.

For this we have presented the Bethe equations for the most general excitation pattern of the uniform light-cone gauged $AdS_5 \times S^5$ superstring in the near plane-wave limit. Moreover, it was demonstrated how excited string states may be translated to distributions of spectral parameters in the Bethe equations as given in table 1. Using this we have explicitly compared the predictions from the light-cone Bethe equations with direct diagonalization of the string Hamiltonian in perturbation theory at leading order in $1/P_+$. For operators from the non dynamical sectors, we have verified the spectrum for a large number of states giving us a strong confidence in the validity of the light-cone Bethe equations for these classes of operators. For a generic $\mathfrak{su}(1, 1|2)$ state, it is much easier to calculate the energy shifts using the Bethe equations. The characteristic polynomial from the perturbative string Hamiltonian is of degree 2^{2K_4} whereas the polynomials needed to be solved in the Bethe equations (4.17) are of degree $K_4 - 2$. Still, one generically deals with polynomials of a high degree, making it hard to explicitly find analytical results for states with large total excitation number K_4 .

When it comes to the dynamical sector $\mathfrak{su}(2|2)$, a direct comparison is much more difficult due to the non linearity and coupled structure of the Bethe equations in (4.17). Here analytical results were established only for the two impurity case. Nevertheless, tests up to impurity number six could be performed numerically.

In the light of this analysis it would be interesting to extend the perturbative study of the string Hamiltonian to next order in $1/P_+$. This is a very complicated problem due to normal ordering ambiguities. However, this problem might be tackled by making use of the symmetry algebra as discussed in [23] and [24]. We hope to return to this issue in the future.

Acknowledgements

We wish to thank Sergey Frolov, Adam Rej, Matthias Staudacher and Tristan McLoughlin for valuable discussions. This work was supported by the Volkswagen-Foundation and the International Max-Planck Research School for Geometric Analysis, Gravitation and String Theory.

Appendix

A. Overview of the string results

To confront the proposed light-cone Bethe equations with the quantum string result

	S_+	S_-	J_+	J_-
$Y_1, P_1^y, \alpha_{1,m}^+, \alpha_{4,m}^-$	0	0	1	1
$Y_2, P_2^y, \alpha_{2,m}^+, \alpha_{3,m}^-$	0	0	1	-1
$Y_3, P_3^y, \alpha_{3,m}^+, \alpha_{2,m}^-$	0	0	-1	1
$Y_4, P_4^y, \alpha_{4,m}^+, \alpha_{1,m}^-$	0	0	-1	-1

	S_+	S_-	J_+	J_-
$Z_1, P_1^z, \beta_{1,m}^+, \beta_{4,m}^-$	1	1	0	0
$Z_2, P_2^z, \beta_{2,m}^+, \beta_{3,m}^-$	1	-1	0	0
$Z_3, P_3^z, \beta_{3,m}^+, \beta_{2,m}^-$	-1	1	0	0
$Z_4, P_4^z, \beta_{4,m}^+, \beta_{1,m}^-$	-1	-1	0	0

	S_+	S_-	J_+	J_-
$\theta_1, \theta_4^\dagger, \theta_{1,m}^+, \theta_{4,m}^-$	0	1	1	0
$\theta_2, \theta_3^\dagger, \theta_{2,m}^+, \theta_{3,m}^-$	0	-1	1	0
$\theta_3, \theta_2^\dagger, \theta_{3,m}^+, \theta_{2,m}^-$	0	1	-1	0
$\theta_4, \theta_1^\dagger, \theta_{4,m}^+, \theta_{1,m}^-$	0	-1	-1	0

	S_+	S_-	J_+	J_-
$\eta_1, \eta_4^\dagger, \eta_{1,m}^+, \eta_{4,m}^-$	1	0	0	1
$\eta_2, \eta_3^\dagger, \eta_{2,m}^+, \eta_{3,m}^-$	1	0	0	-1
$\eta_3, \eta_2^\dagger, \eta_{3,m}^+, \eta_{2,m}^-$	-1	0	0	1
$\eta_4, \eta_1^\dagger, \eta_{4,m}^+, \eta_{1,m}^-$	-1	0	0	-1

Table 9: Charges of the annihilation and creation operators of the $AdS_5 \times S^5$ string in uniform light-cone gauge.

extensive computer algebra computations have been performed to diagonalize the worldsheet Hamiltonian perturbatively. For every considered subsector, i.e. $\mathfrak{su}(2)$, $\mathfrak{sl}(2)$, $\mathfrak{su}(1|1)$, $\mathfrak{su}(1|2)$, $\mathfrak{su}(1, 1|2)$ and $\mathfrak{su}(2|3)$, we state the effective Hamiltonian and present analytic results for its eigenvalues up to three impurities, whenever available. In some cases we had to retreat to a numerical comparison with the Bethe equations, details of these investigations are given in section B.

As one sees in table 1 the total number of impurities (or string excitations) is given by K_4 . We also allow for confluent mode numbers, where the index $k = 1, \dots, K'_4$ counts the excitations with distinct modes, each with a multiplicity of ν_k , using the notation of section 4.2. In uniform light-cone gauge the Hamiltonian eigenvalue $-P_-$ is then given by

$$P_- = - \sum_{k=1}^{K_4} \omega_k + \delta P_- = - \sum_{k=1}^{K'_4} \nu_k \omega_k + \delta P_- \quad (\text{A.1})$$

In order to classify the Hamiltonian eigenvalues we will make use of the $U(1)$ charges $\{S_+, S_-, J_+, J_-\}$ introduced in [23]. They are light-cone combinations of the two spins S_i of AdS_5 and two angular momenta J_i on S^5 , viz. $S_\pm = S_1 \pm S_2$ and $J_\pm = J_1 \pm J_2$. The charges of the string oscillators are spelled out in table 9.

A.1 The $\mathfrak{su}(2)$ sector

This sector consists of states, which are composed only of $\alpha_{1,m}^+$ creation operators. The Hamiltonian (2.11) simplifies dramatically to the effective form

$$\mathcal{H}_4^{(\mathfrak{su}(2))} = \tilde{\lambda} \sum_{\substack{m_1+m_2=0 \\ +m_3+m_4}} \frac{m_2 m_4}{\sqrt{\omega_{m_1} \omega_{m_2} \omega_{m_3} \omega_{m_4}}} \alpha_{1,m_1}^+ \alpha_{1,m_2}^+ \alpha_{1,-m_3}^- \alpha_{1,-m_4}^- \quad . \quad (\text{A.2})$$

This sector is of rank one and the energy shifts $-\delta P_-$ for arbitrary modes m_1, \dots, m_{K_4}

can be evaluated to

$$\delta P_-^{(\mathfrak{su}(2))} = \frac{\tilde{\lambda}}{2P_+} \sum_{\substack{i,j=1 \\ i \neq j}}^{K_4} \frac{(m_i + m_j)^2}{\omega_{m_i} \omega_{m_j}} - \frac{\tilde{\lambda}}{P_+} \sum_{k=1}^{K'_4} \frac{m_k^2}{\omega_{m_k}^2} \nu_k (\nu_k - 1) \quad (\text{A.3})$$

By rewriting this P_- shift in terms of the global energy E and the BMN quantities J and $\lambda' = \lambda/J^2$ using $P_{\pm} = J \pm E$, and then subsequently solving for E one obtains the $\mathfrak{su}(2)$ global energy, which precisely agrees with the results in [20] and [18]

$$E = J + \sum_{k=1}^{K_4} \bar{\omega}_k - \frac{\lambda'}{4J} \sum_{k,j=1}^{K_4} \frac{m_k^2 \bar{\omega}_j^2 + m_j^2 \bar{\omega}_k^2}{\bar{\omega}_k \bar{\omega}_j} - \frac{\lambda'}{4J} \sum_{\substack{i,j=1 \\ i \neq j}}^{K_4} \frac{(m_i + m_j)^2}{\bar{\omega}_i \bar{\omega}_j} + \frac{\lambda'}{2J} \sum_{i=1}^{K'_4} \frac{m_i^2}{\bar{\omega}_i^2} \nu_k (\nu_i - 1)$$

with $\bar{\omega}_k := \sqrt{1 + \lambda' m_k^2}$. (A.4)

A.2 The $\mathfrak{sl}(2)$ sector

The $\mathfrak{sl}(2)$ states are composed of one flavor of $\beta_{1,n}^{\pm}$ operators. Since the structure of the Hamiltonian is identical for $\alpha_{1,n}^{\pm}$ and $\beta_{1,n}^{\pm}$ up to a minus sign one immediately has

$$\mathcal{H}_4^{(\mathfrak{sl}(2))} = -\tilde{\lambda} \sum_{\substack{m_1+m_2=0 \\ +m_3+m_4}} \frac{m_2 m_4}{\sqrt{\omega_{m_1} \omega_{m_2} \omega_{m_3} \omega_{m_4}}} \beta_{1,m_1}^+ \beta_{1,m_2}^+ \beta_{1,-m_3}^- \beta_{1,-m_4}^- \quad (\text{A.5})$$

$$\delta P_-^{(\mathfrak{sl}(2))} = -\delta P_-^{(\mathfrak{su}(2))} \quad (\text{A.6})$$

and the global energy shift follows immediately.

A.3 The $\mathfrak{su}(1|1)$ sector

States of the $\mathfrak{su}(1|1)$ sector are formed of $\theta_{1,n}^{\pm}$ creation operators. As noted in [23] the restriction of the $\mathcal{O}(1/P_+)$ string Hamiltonian (2.11) to the pure $\mathfrak{su}(1|1)$ sector vanishes

$$\mathcal{H}_4^{(\mathfrak{su}(1|1))} \equiv 0, \quad \delta P_-^{(\mathfrak{su}(1|1))} = 0. \quad (\text{A.7})$$

A.4 The $\mathfrak{su}(1|2)$ sector

We now turn to the first larger rank sector $\mathfrak{su}(1|2)$ being spanned by the creation operators $\theta_{1,n}^+$ and $\alpha_{1,n}^+$ of one flavor. The effective Hamiltonian is given by

$$\mathcal{H}_4^{(\mathfrak{su}(1|2))} = \mathcal{H}_4^{(\mathfrak{su}(2))} + \tilde{\lambda} \sum_{\substack{m_1+m_2=0 \\ +m_3+m_4}} \frac{X(m_1, m_2, m_3, m_4)}{\sqrt{\omega_{m_3} \omega_{m_4}}} \theta_{1,m_1}^+ \theta_{1,-m_2}^- \alpha_{1,m_3}^+ \alpha_{1,-m_4}^- \quad (\text{A.8})$$

where $X(m, n, k, l)$ is defined as

$$X(m, n, k, l) := \left[\left(mn - \frac{(m-n)(k-l)}{4} \right) (f_n f_m + g_n g_m) - \frac{\kappa}{4\sqrt{\tilde{\lambda}}} (k+l) (\omega_k + \omega_l) (f_n g_m + f_m g_n) \right], \quad (\text{A.9})$$

where $\kappa = \pm 1$.

A.4.1 Two impurities

For two impurity $\mathfrak{su}(1|2)$ states carrying the modes $m_1 = -m_2$ the Hamiltonian \mathcal{H}_4 forms a 4×4 matrix with eigenvalues $-\delta P_-$ where

$$\delta P_- = \left\{ \pm 2 \frac{\tilde{\lambda}}{P_+} \frac{m_1^2}{\omega_1}, 0, 0 \right\}. \quad (\text{A.10})$$

A.4.2 Three impurities with distinct modes

Considering the three impurity case with distinct mode numbers m_1, m_2, m_3 the Hamiltonian is represented by an 8×8 matrix which decomposes into 4 non mixing submatrices, where two fall into the rank one sectors $\mathfrak{su}(2)$ and $\mathfrak{su}(1|1)$. The remaining pieces are two 3×3 matrices.

Since string states only mix if they carry the same charges, we can classify the submatrices and their eigenvalues by the charge of the corresponding states. One finds:

$$\{S_+, S_-, J_+, J_-\} = \{0, 2, 3, 1\}_{\theta_1^+ \alpha_1^+ \alpha_1^+ | 0} :$$

$$\delta P_- = \left\{ \pm \frac{\tilde{\lambda}}{P_+} \sum_{j=1}^3 \frac{m_j^2}{\omega_j}, \frac{\tilde{\lambda}}{P_+ \omega_1 \omega_2 \omega_3} \sum_{j=1}^3 m_j^2 \omega_j \right\} \quad (\text{A.11})$$

$$\{S_+, S_-, J_+, J_-\} = \{0, 1, 3, 2\}_{\theta_1^+ \alpha_1^+ \alpha_1^+ | 0} :$$

$$\delta P_- = \left\{ 0, \frac{\tilde{\lambda}}{P_+} \frac{m_1^2 \omega_{m_1} + m_2^2 \omega_{m_2} + m_3^2 \omega_{m_3} \pm \Xi_{m_1, m_2, m_3}}{\omega_{m_1} \omega_{m_2} \omega_{m_3}} \right\} \quad (\text{A.12})$$

$$\text{with } \Xi_{a,b,c} := \sqrt{4(\omega_a^2 \chi_{b,c}^2 + \omega_b^2 \chi_{a,c}^2 + \omega_c^2 \chi_{a,b}^2) + (\xi_{a,b,c} - \xi_{b,a,c} + \xi_{c,a,b})^2 - 4\xi_{a;b,c} \xi_{c;a,b}}$$

$$\xi_{a;b,c} := -a(b\omega_b + c\omega_c - a\omega_a)$$

$$\chi_{a,b} := -ab \frac{\tilde{\lambda} ab - (1 + \omega_a)(1 + \omega_b)}{\sqrt{(1 + \omega_a)(1 + \omega_b)}}.$$

A.4.3 Three impurities with confluent modes

In the case of confluent modes $\{m_1, m_2, m_3\} = \{m, m, -2m\}$ the submatrix with charges $\{0, 2, 3, 1\}$ collapses to a scalar whereas the submatrix of charge $\{0, 1, 3, 2\}$ reduces to 2×2 matrix with energy shifts

$$\{S_+, S_-, J_+, J_-\} = \{0, 2, 3, 1\}_{\theta_1^+ \alpha_1^+ \alpha_1^+ | 0} : \quad \delta P_- = \frac{\tilde{\lambda}}{P_+} \frac{2m^2}{\omega_m} \left(\frac{1}{\omega_m} + \frac{1}{\omega_{2m}} \right) \quad (\text{A.13})$$

$$\{S_+, S_-, J_+, J_-\} = \{0, 1, 3, 2\}_{\theta_1^+ \alpha_1^+ \alpha_1^+ | 0} : \quad (\text{A.14})$$

$$\delta P_- = 2 \frac{\tilde{\lambda} q^2}{P_+ \omega_q^2 \omega_{2q}} \left(\omega_q + \omega_{2q} \pm \omega_q \sqrt{3 + 2\omega_{2q}^2 + 4\omega_q \omega_{2q}} \right)$$

A.5 The $\mathfrak{su}(1, 1|2)$ sector

States of the $\mathfrak{su}(1, 1|2)$ sector are spanned by the set $\{\theta_{1,n}^+, \eta_{1,n}^+, \beta_{1,n}^+, \alpha_{1,n}^+\}$ of creation operators. In this sector the effective Hamiltonian takes the form

$$\begin{aligned}
\mathcal{H}_4^{(\mathfrak{su}(1,1|2))} &= \tilde{\lambda} \sum_{\substack{k+l \\ +n+m=0}} \frac{kl}{\sqrt{\omega_m \omega_n \omega_k \omega_l}} (\alpha_{1,m}^+ \alpha_{1,-n}^- - \beta_{1,m}^+ \beta_{1,-n}^-) (\alpha_{1,k}^+ \alpha_{1,-l}^- + \beta_{1,k}^+ \beta_{1,-l}^-) \\
&+ \tilde{\lambda} \sum_{\substack{k+l \\ +n+m=0}} 2i \frac{f_m f_n - g_m g_n}{\sqrt{\omega_k \omega_l}} (\theta_{1,m}^+ \eta_{1,n}^+ \beta_{1,-k}^- \alpha_{1,-l}^- + \theta_{1,-m}^- \eta_{1,-n}^- \beta_{1,k}^+ \alpha_{1,l}^+) \\
&+ \tilde{\lambda} \sum_{\substack{k+l \\ +n+m=0}} \frac{X(m, n, k, l)}{\sqrt{\omega_k \omega_l}} (\theta_{1,m}^+ \theta_{1,-n}^- + \eta_{1,m}^+ \eta_{1,-n}^-) (\alpha_{1,k}^+ \alpha_{1,-l}^- - \beta_{1,k}^+ \beta_{1,-l}^-),
\end{aligned} \tag{A.15}$$

where $X(m, n, k, l)$ is given in (A.9).

A.5.1 Two impurities

The Hamiltonian matrix decomposes into several non mixing submatrices. The $\mathfrak{su}(1, 1|2)$ sector contains all previous discussed sectors, whose eigenvalues we do not state again. For the two impurity case with mode numbers $m_1 = -m_2$ one obtains the new eigenvalues:

$$\{1, 1, 1, 1\}_{\theta_1^+ \eta_1^+ | 0}, \beta_1^+ \alpha_1^+ | 0} : \quad \delta P_- = \left\{ \pm 4 \frac{\tilde{\lambda}}{P_+} \frac{m_1^2}{\omega_1}, 0, 0 \right\} \tag{A.16}$$

$$\begin{aligned}
&\{1, 2, 1, 0\}_{\theta_1^+ \beta_1^+ | 0}, \{0, 1, 2, 1\}_{\theta_1^+ \alpha_1^+ | 0} \\
&\{2, 1, 0, 1\}_{\eta_1^+ \beta_1^+ | 0}, \{1, 0, 1, 2\}_{\eta_1^+ \alpha_1^+ | 0}
\end{aligned} \quad \delta P_- = \pm 2 \frac{\tilde{\lambda}}{P_+} \frac{m_1^2}{\omega_1} \tag{A.17}$$

A.5.2 Three impurities with confluent modes

For higher impurities the situation becomes much more involved. Already the three impurity $\mathfrak{su}(1, 1|2)$ Hamiltonian for non-confluent modes becomes a 64×64 matrix with submatrices of rank 9. We will classify the $\mathfrak{su}(1, 1|2)$ submatrices with respect to their charges and dimension d . Because $\mathfrak{su}(1, 1|2)$ contains previously discussed sectors, we can deduce most of the eigenvalues by using properties of the Hamiltonian $\mathcal{H}_4^{(\mathfrak{su}(1,1|2))}$. Our findings are collected in the table 10.

The structure of the 9×9 submatrices is a bit more involved. Under the oscillator exchange $\theta_{1,m} \leftrightarrow \eta_{1,m}$ and $\alpha_{1,m} \leftrightarrow \beta_{1,m}$ the effective Hamiltonian $\mathcal{H}_4^{(\mathfrak{su}(1,1|2))}$ changes its sign. This exchange translates a state with charge $\{1, 1, 2, 2\}$ into one with $\{2, 2, 1, 1\}$ or a $\{1, 2, 2, 1\}$ charged state into one with $\{2, 1, 1, 2\}$ and vice versa with mutual energy shifts of opposite signs. See table 11 for results.

dimension $d = 1$

$\{S_+, S_-, J_+, J_-\}$	State pattern	Property	δP_-
$\{0, 0, 3, 3\}$	$\alpha_1^+ \alpha_1^+ \alpha_1^+ 0\rangle$	$\mathfrak{su}(2)$ state	(A.3)
$\{3, 3, 0, 0\}$	$\beta_1^+ \beta_1^+ \beta_1^+ 0\rangle$	$\mathfrak{sl}(2)$ state	(A.6)

dimension $d = 3$

$\{S_+, S_-, J_+, J_-\}$	State pattern	Property	δP_-
$\{0, 2, 3, 1\}$	$\theta_1^+ \theta_1^+ \alpha_1^+ 0\rangle$	$\mathfrak{su}(1 2)$ state	$\delta P_-^{\{0,2,3,1\}}$ see (A.11)
$\{2, 0, 1, 3\}$	$\eta_1^+ \eta_1^+ \alpha_1^+ 0\rangle$	property of (A.15) implies	$\delta P_-^{\{2,1,0,3\}} = +\delta P_-^{\{0,2,3,1\}}$
$\{1, 3, 2, 0\}$	$\theta_1^+ \theta_1^+ \beta_1^+ 0\rangle$	property of (A.15) implies	$\delta P_-^{\{1,3,2,0\}} = -\delta P_-^{\{0,2,3,1\}}$
$\{3, 1, 0, 2\}$	$\eta_1^+ \eta_1^+ \beta_1^+ 0\rangle$	property of (A.15) implies	$\delta P_-^{\{3,1,0,2\}} = -\delta P_-^{\{0,2,3,1\}}$
$\{0, 1, 3, 2\}$	$\theta_1^+ \alpha_1^+ \alpha_1^+ 0\rangle$	$\mathfrak{su}(1 2)$ state	$\delta P_-^{\{0,1,3,2\}}$ see (A.12)
$\{1, 0, 2, 3\}$	$\eta_1^+ \alpha_1^+ \alpha_1^+ 0\rangle$	property of (A.15) implies	$\delta P_-^{\{1,0,2,3\}} = +\delta P_-^{\{0,1,3,2\}}$
$\{2, 3, 1, 0\}$	$\theta_1^+ \beta_1^+ \beta_1^+ 0\rangle$	property of (A.15) implies	$\delta P_-^{\{2,3,1,0\}} = -\delta P_-^{\{0,1,3,2\}}$
$\{3, 2, 0, 1\}$	$\eta_1^+ \beta_1^+ \beta_1^+ 0\rangle$	property of (A.15) implies	$\delta P_-^{\{3,2,0,1\}} = -\delta P_-^{\{0,1,3,2\}}$

Table 10: Analytically accessible three impurity, distinct $\mathfrak{su}(1, 1|2)$ energy shifts.

A.6 The $\mathfrak{su}(2|3)$ sector

Finally the $\mathfrak{su}(2|3)$ sector is spanned by the operators $\theta_{1,n}^+, \theta_{2,n}^+, \alpha_{1,n}^+, \alpha_{2,n}^+$. The effective form of \mathcal{H}_4 in this closed subsector reads

$$\begin{aligned}
\mathcal{H}_4^{(\mathfrak{su}(2|3))} = & \\
& \tilde{\lambda} \sum_{\substack{k+l \\ +n+m=0}} \frac{k l}{\sqrt{\omega_m \omega_n \omega_k \omega_l}} (\alpha_{1,m}^+ \alpha_{1,-n}^- + \alpha_{2,m}^+ \alpha_{2,-n}^-) (\alpha_{1,k}^+ \alpha_{1,-l}^- + \alpha_{2,k}^+ \alpha_{2,-l}^-) \\
& + \tilde{\lambda} \sum_{\substack{k+l \\ +n+m=0}} \frac{X(m, n, k, l)}{\sqrt{\omega_k \omega_l}} (\theta_{1,m}^+ \theta_{1,-n}^- + \theta_{2,m}^+ \theta_{2,-n}^-) (\alpha_{1,k}^+ \alpha_{1,-l}^- + \alpha_{2,k}^+ \alpha_{2,-l}^-) \quad (\text{A.18}) \\
& - \frac{\tilde{\lambda}}{2} \text{i} \sum_{\substack{k+l \\ +n+m=0}} \frac{1}{\sqrt{\omega_k \omega_l}} (\theta_{2,m}^+ \theta_{1,n}^+ \alpha_{2,-k}^- \alpha_{1,-l}^- + \theta_{2,-m}^- \theta_{1,-n}^- \alpha_{2,k}^+ \alpha_{1,l}^+) \\
& \quad \times \left[(m-n)(k-l)(f_n g_m - f_m g_n) + \frac{\kappa}{\sqrt{\lambda}} (k+l)(\omega_k - \omega_l)(f_n f_m - g_m g_n) \right] \\
& + \tilde{\lambda} \sum_{\substack{k+l \\ +n+m=0}} \left(\begin{array}{l} (f_m g_n + f_n g_m)(f_k g_l + f_l g_k)(mn + kl) \\ + (f_n g_k + f_k g_n)(f_m g_l + f_l g_m)(nk + ml) \\ - (f_n f_l - g_n g_l)(f_m f_k + g_m g_k)(nl + mk) \end{array} \right) \theta_{2,m}^+ \theta_{2,-n}^- \theta_{1,k}^+ \theta_{1,-l}^- .
\end{aligned}$$

dimension $d = 9$

$\{S_+, S_-, J_+, J_-\}$	State pattern	δP_-
$\{1, 1, 2, 2\}$	$\beta_1^+ \alpha_1^+ \alpha_1^+ 0\rangle, \theta_1^+ \eta_1^+ \alpha_1^+ 0\rangle$	rank 9 matrix, numerical eigenvalues see table 12
$\{2, 2, 1, 1\}$	$\beta_1^+ \beta_1^+ \alpha_1^+ 0\rangle, \theta_1^+ \eta_1^+ \beta_1^+ 0\rangle$	$\delta P_-^{\{2,2,1,1\}} = -\delta P_-^{\{1,1,2,2\}}$
$\{1, 2, 2, 1\}$	$\theta_1^+ \theta_1^+ \eta_1^+ 0\rangle, \theta_1^+ \beta_1^+ \alpha_1^+ 0\rangle$	rank 6 matrix, numerical eigenvalues see table 12
$\{2, 1, 1, 2\}$	$\theta_1^+ \eta_1^+ \eta_1^+ 0\rangle, \eta_1^+ \beta_1^+ \alpha_1^+ 0\rangle$	$\delta P_-^{\{2,1,1,2\}} = -\delta P_-^{\{1,2,2,1\}}$

Table 11: Remaining three impurity, distinct $\mathfrak{su}(1,1|2)$ shifts, which were compared numerically.

A.6.1 Two impurities

For two impurities with mode numbers $m_2 = -m_1$ we find the energy shifts

$$\{0, 0, 2, 0\}_{\theta_2^+ \theta_1^+ |0\rangle, \alpha_2^+ \alpha_1^+ |0\rangle} : \quad \delta P_- = \left\{ \pm 4 \frac{\tilde{\lambda}}{P_+} \frac{m_1^2}{\omega_1}, 0, 0 \right\} \quad (\text{A.19})$$

$$\begin{aligned} & \{0, 1, 2, 1\}_{\theta_1^+ \alpha_1^+ |0\rangle}, \quad \{0, 1, 2, -1\}_{\theta_1^+ \alpha_2^+ |0\rangle} \\ & \{0, -1, 2, 1\}_{\theta_2^+ \alpha_1^+ |0\rangle}, \quad \{0, -1, 2, -1\}_{\theta_2^+ \alpha_2^+ |0\rangle} \end{aligned} \quad \delta P_- = \pm 2 \frac{\tilde{\lambda}}{P_+} \frac{m_1^2}{\omega_1} \quad (\text{A.20})$$

B. Numerical results

Here we collect the numerical results, for this we dial explicit mode numbers and values for the coupling constant λ' . The considered cases constitute certain three impurity excitations in the $\mathfrak{su}(1,1|2)$ subsector with distinct and confluent mode numbers, as well as all three impurity excitations (distinct and confluent) for the $\mathfrak{su}(2|3)$ subsector. In the tables below we state explicit results for the values $\tilde{\lambda} = 0.1$ and $P_+ = 100$ and mode numbers $(m_1, m_2, m_3) = \{(2, 1, -3), (3, 3, -6)\}$. All numerical energy shifts were matched precisely with the result obtained from the Bethe equations.

⁸The \pm signs at some charges are just a shortform of writing several charge combinations all with the same eigenvalues. They are not related to the signatures of the eigenvalues in any sense.

$\mathfrak{su}(2|3)$ sector⁸

$\{S_+, S_-, J_+, J_-\}$	eigenvalues $-\delta P_-$				
$\{0,0,3,\pm 3\}$	-0.0106324				
$\{0,\pm 2,3,\pm 1\}$	± 0.0108634	-0.0106324			
$\{0,\pm 1,3,\pm 2\}$	-0.0214958	0.000230962	0		
$\{0,\pm 1,3,0\}$	0.0217267	3×-0.0214958	2×0.000230962	3×0	
$\{0,0,3,\pm 1\}$	-0.0323591	0.0110943	$2 \times \pm 0.0108634$	3×-0.0106324	

$\mathfrak{su}(1,1|2)$ sector

$\{S_+, S_-, J_+, J_-\}$	eigenvalues $-\delta P_-$				
$\{1,1,2,2\}$	-0.0323591	0.0110943	$2 \times \pm 0.0108634$	2×-0.0106324	0.0106324
$\{1,2,2,1\}, \{2,1,1,2\}$	± 0.0217267	± 0.0214958	± 0.000230962	3×0	
$\{2,2,1,1\}$	0.0323591	-0.0110943	$2 \times \pm 0.0108634$	2×0.0106324	-0.0106324

Table 12: Numerical results for the first order correction in $1/P_+$ of the string energy spectrum for three impurity states with distinct mode numbers $m_1 = 2, m_2 = 1, m_3 = -3$. The number in front of some eigenvalues denotes their multiplicity if unequal to one.

$\mathfrak{su}(2|3)$ sector

$\{S_+, S_-, J_+, J_-\}$	eigenvalues $-\delta P_-$		
$\{0,\pm 1,3,0\}$	2×-0.0454059	2×0.0142814	
$\{0,0,3,\pm 1\}$	-0.0752496	0.044125	3×-0.0155623
$\{0,\pm 2,3,\pm 1\}, \{0,0,3,\pm 3\}$	-0.0155623		
$\{0,\pm 1,3,\pm 2\}$	-0.0454059	0.0142814	

$\mathfrak{su}(1,1|2)$ sector

$\{S_+, S_-, J_+, J_-\}$	eigenvalues $-\delta P_-$			
$\{1,1,2,2\}$	-0.0752496	0.044125	0.0155623	2×-0.0155623
$\{1,2,2,1\}, \{2,1,1,2\}$	± 0.0454059	± 0.0142814		
$\{2,2,1,1\}$	0.0752496	-0.044125	2×0.0155623	-0.0155623

Table 13: Numerical results for the first order correction in $1/P_+$ of the string energy spectrum for three impurity states with confluent mode numbers $m_1 = m_2 = 3, m_3 = -6$. The number in front of some eigenvalues denotes their multiplicity if unequal to one.

References

- [1] R. R. Metsaev and A. A. Tseytlin, “Type IIB superstring action in $\text{AdS}_5 \times S^5$ background,” Nucl. Phys. B **533** (1998) 109, hep-th/9805028.
- [2] J. M. Maldacena, “The large N limit of superconformal field theories and supergravity,” Adv. Theor. Math. Phys. **2**, 231 (1998) [Int. J. Theor. Phys. **38**, 1113 (1999)], hep-th/9711200. • S. S. Gubser, I. R. Klebanov and A. M. Polyakov, “Gauge theory correlators from non-critical string theory,” Phys. Lett. B **428** (1998) 105, hep-th/9802109. • E. Witten, “Anti-de Sitter space and holography,” Adv. Theor. Math. Phys. **2**, 253 (1998), hep-th/9802150.
- [3] J. A. Minahan and K. Zarembo, “The Bethe-ansatz for $N = 4$ super Yang-Mills,” JHEP **0303**, 013 (2003), hep-th/0212208.

- [4] N. Beisert, “The dilatation operator of $N = 4$ super Yang-Mills theory and integrability,” *Phys. Rept.* **405** (2005) 1, hep-th/0407277 • K. Zarembo, “Semiclassical Bethe ansatz and AdS/CFT,” *Comptes Rendus Physique* **5** (2004) 1081 [*Fortsch. Phys.* **53** (2005) 647], hep-th/0411191 • J. Plefka, “Spinning strings and integrable spin chains in the AdS/CFT correspondence,” *Living Rev. in Relativity* **8**, (2005), hep-th/0507136. • J. A. Minahan, “A Brief Introduction To The Bethe Ansatz In $N=4$ Super-Yang-Mills,” *J. Phys. A* **39** (2006) 12657.
- [5] N. Beisert, C. Kristjansen and M. Staudacher, “The dilatation operator of $N = 4$ super Yang-Mills theory,” *Nucl. Phys. B* **664** (2003) 131, hep-th/0303060. • N. Beisert and M. Staudacher, “The $N = 4$ SYM integrable super spin chain,” *Nucl. Phys. B* **670** (2003) 439, hep-th/0307042.
- [6] N. Beisert, V. A. Kazakov, K. Sakai and K. Zarembo, “Complete spectrum of long operators in $N = 4$ SYM at one loop,” *JHEP* **0507** (2005) 030, hep-th/0503200.
- [7] N. Beisert and M. Staudacher, “Long-range PSU(2,2|4) Bethe ansätze for gauge theory and strings,” *Nucl. Phys. B* **727** (2005) 1, hep-th/0504190.
- [8] M. Staudacher, “The factorized S-matrix of CFT/AdS,” *JHEP* **0505** (2005) 054, hep-th/0412188.
- [9] N. Beisert, “The su(2|2) dynamic S-matrix,” hep-th/0511082.
- [10] R. A. Janik, “The $AdS_5 \times S^5$ superstring worldsheet S-matrix and crossing symmetry,” *Phys. Rev. D* **73** (2006) 086006, hep-th/0603038.
- [11] C. Gomez and R. Hernandez, “The magnon kinematics of the AdS/CFT correspondence,” *JHEP* **0611** (2006) 021, hep-th/0608029. • J. Plefka, F. Spill and A. Torrielli, “On the Hopf algebra structure of the AdS/CFT S-matrix,” *Phys. Rev. D* **74** (2006) 066008, hep-th/0608038.
- [12] N. Beisert, R. Hernandez and E. Lopez, “A crossing-symmetric phase for $AdS_5 \times S^5$ strings,” *JHEP* **0611** (2006) 070, hep-th/0609044. • N. Beisert, B. Eden and M. Staudacher, “Transcendentality and crossing,” *J. Stat. Mech.* **0701** (2007) P021, hep-th/0610251.
- [13] Z. Bern, M. Czakon, L. J. Dixon, D. A. Kosower and V. A. Smirnov, “The four-loop planar amplitude and cusp anomalous dimension in maximally supersymmetric Yang-Mills theory,” hep-th/0610248. • F. Cachazo, M. Spradlin and A. Volovich, “Four-loop cusp anomalous dimension from obstructions,” hep-th/0612309.
- [14] I. Bena, J. Polchinski and R. Roiban, “Hidden symmetries of the $AdS_5 \times S^5$ superstring,” *Phys. Rev. D* **69** (2004) 046002, hep-th/0305116.
- [15] D. M. Hofman and J. M. Maldacena, “Giant magnons,” *J. Phys. A* **39** (2006) 13095, hep-th/0604135.

- [16] D. Berenstein, J. M. Maldacena and H. Nastase, “Strings in flat space and pp waves from $N = 4$ super Yang Mills,” *JHEP* **0204**, 013 (2002), hep-th/0202021.
- [17] C. G. Callan, H. K. Lee, T. McLoughlin, J. H. Schwarz, I. Swanson and X. Wu, “Quantizing string theory in $AdS_5 \times S^5$: Beyond the pp-wave,” *Nucl. Phys. B* **673** (2003) 3, hep-th/0307032. • C. G. Callan, T. McLoughlin and I. Swanson, “Holography beyond the Penrose limit,” *Nucl. Phys. B* **694** (2004) 115, hep-th/0404007. • C. G. Callan, T. McLoughlin and I. J. Swanson, “Higher impurity AdS/CFT correspondence in the near-BMN limit,” *Nucl. Phys. B* **700** (2004) 271, hep-th/0405153].
- [18] T. McLoughlin and I. J. Swanson, “N-impurity superstring spectra near the pp-wave limit,” *Nucl. Phys. B* **702** (2004) 86, hep-th/0407240.
- [19] M. J. Martins and C. S. Melo, “The spectrum of particles interacting through centrally extended $su(2|2)$ S-matrices,” hep-th/0703086.
- [20] G. Arutyunov, S. Frolov and M. Staudacher, “Bethe ansatz for quantum strings,” *JHEP* **0410**, 016 (2004), hep-th/0406256.
- [21] G. Arutyunov and S. Frolov, “Integrable Hamiltonian for classical strings on $AdS_5 \times S^5$,” *JHEP* **0502** (2005) 059, hep-th/0411089.
- [22] G. Arutyunov and S. Frolov, “Uniform light-cone gauge for strings in $AdS_5 \times S^5$: Solving $su(1|1)$ sector,” *JHEP* **0601** (2006) 055, hep-th/0510208.
- [23] S. Frolov, J. Plefka and M. Zamaklar, “The $AdS_5 \times S^5$ superstring in light-cone gauge and its Bethe equations,” *J. Phys. A* **39** (2006) 1303, hep-th/0603008.
- [24] G. Arutyunov, S. Frolov, J. Plefka and M. Zamaklar, “The off-shell symmetry algebra of the light-cone $AdS_5 \times S^5$ superstring,” hep-th/0609157.
- [25] G. Arutyunov, S. Frolov and M. Zamaklar, “The Zamolodchikov-Faddeev algebra for $AdS_5 \times S^5$ superstring,” hep-th/0612229.
- [26] T. Klose, T. McLoughlin, R. Roiban and K. Zarembo, “Worldsheet scattering in $AdS_5 \times S^5$,” hep-th/0611169.
- [27] T. Klose and K. Zarembo, “Bethe ansatz in stringy sigma models,” *J. Stat. Mech.* **0605** (2006) P006, hep-th/0603039. • T. Klose and K. Zarembo, “Reduced sigma-model on $AdS_5 \times S^5$: One-loop scattering amplitudes,” *JHEP* **0702** (2007) 071, hep-th/0701240.
- [28] G. Arutyunov and S. Frolov, “On $AdS_5 \times S^5$ string S-matrix,” *Phys. Lett. B* **639** (2006) 378, hep-th/0604043.
- [29] C.-N. Yang, “Some exact results for the many body problems in one dimension with repulsive delta function interaction,” *Phys. Rev Lett.* **19**, 1312 (1967).

- [30] T. J. Stieltjes. "Sur Quelques Theoremes d'Algebre," *Ouvres Completes*. vol. 1, p 440, Noordhoff, Groningen, The Netherlands (1914) • B. S. Shastri. A. Dhar, "Solution of a generalized Stieltjes Problem" *J. Phys A* **34** (2001) 6197-6208, cond-mat/0101464.